Chem Soc Rev

REVIEW ARTICLE

View Article Online
View Journal | View Issue

Cite this: *Chem. Soc. Rev.*, 2020, **49**, 6733

Where silylene–silicon centres matter in the activation of small molecules

Changkai Shan, Shenglai Yao and Matthias Driess *

Small molecules such as H_2, N_2, CO, NH_3, O_2 are ubiquitous stable species and their activation and role in the formation of value-added products are of fundamental importance in nature and industry. The last few decades have witnessed significant advances in the chemistry of heavy low-coordinate main-group elements, with a plethora of newly synthesised functional compounds, behaving like transition-metal complexes with respect to facile activation of such small molecules. Among them, silylenes have received particular attention in this vivid area of research showing even metal-free bond activation and catalysis. Recent striking discoveries in the chemistry of silylenes take advantage of narrow HOMO–LUMO energy gap and Lewis acid–base bifunctionality of divalent Si centres. The review is devoted to recent advances of using isolable silylenes and corresponding silylene–metal complexes for the activation of fundamental but inert molecules such as H_2, CO_x, N_2O, O_2, H_2O, NH_3, C_2H_4 and E_4 (E = P, As).

Received 29th June 2020

DOI: 10.1039/d0cs00815j

rsc.li/chem-soc-rev

1. Introduction

Nowadays, small molecules such as H_2, CO_x, N_2O, O_2, H_2O, *etc.* are ubiquitous as well as economically available building blocks for fundamental chemical processes in the production of value-added fine chemicals and play a pivotal role in maintaining the prospects of industrial society.[1] They are very stable, that is, the activation of their relatively inert bonds for selective chemical transformations requires a suitable catalyst. Learning from biocatalysts in nature and taking advantage of new synthetic methods in organometallic and coordination chemistry have paved the way to numerous artificial molecular catalysts for selective activation and transformation of small molecules.

1.1 Activation of small molecules in nature

Nature has developed a myriad of cellular enzymes, the majority of which harbour a transition-metal cofactor and are capable of small-molecule conversion with high efficiency under mild conditions.[2] For example, nitrogenase, one of the most important enzymes, allows for dinitrogen fixation and further synthesis of fundamental building blocks of cellular molecules.

Department of Chemistry, Metalorganics and Inorganic Materials, Technische Universität Berlin, Strasse des 17. Juni 135, Sekr. C2, 10623 Berlin, Germany. E-mail: matthias.driess@tu-berlin.de

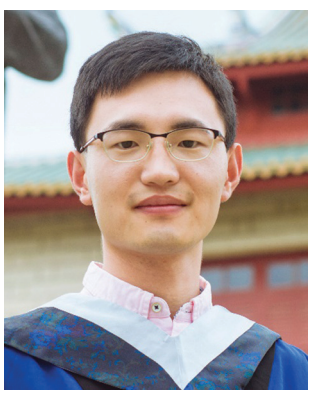

Changkai Shan

Changkai Shan is currently a PhD candidate under the supervision of Prof. Matthias Driess at the Department of Metalorganics and Inorganic Materials, Technical University of Berlin. He received his MSc in organic chemistry from Xiamen University, China in 2018. His current research focuses on the synthesis of novel silylene-ligands and their reactivity towards catalysis and small molecule activation.

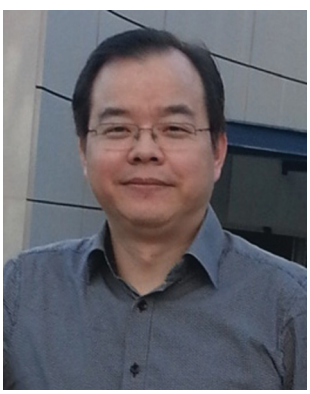

Shenglai Yao

Shenglai Yao attained his PhD degree in 2005 at the Johannes Gutenberg University of Mainz (Germany) under supervision of Professor Karl W. Klinkhammer. Afterwards he joined the Driess group at the Department of Metalorganics and Inorganic Materials, Technical University of Berlin and works in the group as a senior researcher. His research interests lie in the coordination chemistry of low-valent main-group elements and transition metals.

The molybdenum-dependent nitrogenase consists of electron-delivery protein components and MoFe cofactor, where N_2 is reduced to NH_3. At the same time, vanadium-dependent or heterometal-independent forms show less reactivity.[3] Hydrogenases are remarkable catalysts for reversible H_2 oxidation and proton reduction along with an energy-yielding process. They can be divided into two major classes, namely [NiFe]- and [FeFe]-hydrogenases.[3b,4] H_2O and O_2 are essential components in both photosystem II (PSII) and cytochromes P450 (P450). PSII, a metal-bound protein complex, catalyses the light-driven oxidation of water by taking advantage of the four-electron redox-active Mn_4CaO_5 cluster,[5] whereas P450 catalyses the introduction of O_2 into non-activated C–H bonds with the assistance of a protein partner to deliver one or more electrons to the Fe reactive site.[6] CO dehydrogenase (CODH) with a [Ni4Fe–5S] or [4Fe–4S] cluster can convert CO_2 to the more valuable synthetic feedstock CO.[7] Taking the aforementioned few examples as an inspiration for synthetic chemists, the design of artificial catalysts that are approximate to or even better than their natural counterparts is highly desirable.

1.2 Artificial transition-metal-mediated activation of small molecules

Coordination chemists were much inspired by biocatalysis and developed an enormous number of artificial metalloenzymes for small molecule activation (*e.g.*, oxygenases, hydrogenases, carboxodehydrogenases, nitrogenases) mimicking their counterparts in nature.[8] To mention only a few selected ones, artificial metalloenzymes consisting of Fe or Mn centres have been synthesised for O_2 activation;[9] for example, the well-known O_2-dependent phenol oxidase **A** (Fig. 1), bearing a "Due Ferri" (two-iron; DF) diiron cofactor, is capable to catalyse the oxidative transformation of 4-aminophenol to the corresponding quinone monoimine.[10] Mimicking photosystem II (PSII), among many other examples, a molecular dinuclear Mn_2H_5L cluster allows for photocatalytic oxygen evolution reaction (OER) from water oxidation.[11] Oxidation of H_2 seems more complex than its back reaction (hydrogen evolution reaction (HER) from water reduction).[12] In this regard, the designed diiron complex **B** (Fig. 1), modelling [FeFe] hydrogenase, participates in the oxidation of H_2 only with a slow conversion rate.[13] CO_2 is the primary C_1 source in nature and the electrochemical reduction of CO_2 with, for example, $[Ni^{II}(cyclam)]^{2+}$ (cyclam = 1,4,8,11-tetraazacyclotetradecane) **C** (Fig. 1), affords CO in aqueous and dimethylformamide (DMF) solutions.[11] Notably, many synthetic Fe–S clusters mimicking nitrogenases have been reported, and these artificial clusters may one day approximate or surpass the ability of natural nitrogenases on the fixation and conversion of N_2.[14]

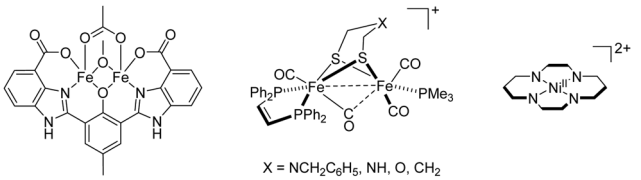

A B C

Fig. 1 Examples of artificial metalloenzyme cofactors **A**, **B** and **C** (four protons on the N atoms are omitted for clarity).

1.3 Main-group elements mimicking transition-metals in small molecule activation

The seminal review entitled "Main-Group Elements as Transition Metals" published by Power[15] reflected a renaissance of main-group chemistry aiming at the development of even metal-free, benign catalysts as alternative mediators for the synthesis of fine chemicals compared to those relying on transition-metals. At first, the valence s or p orbitals of main-group compounds are thought to be far apart energetically. However, dozens of isolable low-coordinate main-group species exist, possessing frontier orbitals with small-energy separations, which show transition-metal-like properties towards small molecules.[16] A striking example for the activation of H_2 was reported by Power in 2005, where a heavy alkyne analogue with Ge [Ge≡Ge; Ar = 2,6-$Trip_2$-C_6H_3 (Trip = 2,4,6-$^iPr_3C_6H_2$)] splits the H–H bond at room temperature to give Ar(H)Ge═Ge(H)Ar, $Ar(H)_2Ge$–$Ge(H)_2Ar$, and $ArGeH_3$, respectively.[17] Electron donation from the σ-orbital of H_2 into the LUMO of the Ge species as well as a synergistic electron donation from the π-HOMO of the Ge species into the σ*-orbital of H_2 are involved in the disruption of H–H bond, reminiscent of interactions between H_2 and a transition-metal site in complexes (Fig. 2). Bertrand also showed that acyclic alkyl amino carbenes (aCAAC), such as [:C(*t*Bu)N^{i}Pr$_2$], can readily break the H–H bond to give the corresponding [H_2C(*t*Bu)N^{i}Pr$_2$] addition product.[18] Related stable carbenes also take part in the activation of unactivated bonds, acting also as ligands towards transition metals for the stabilisation of reactive intermediates.[19] Stephan *et al.* reported the activation of H_2 by the use of frustrated Lewis pairs (FLPs). FLPs bearing both an available acceptor and donor orbitals mimic a similar function of frontier orbitals in transition-metal complexes.[20] Singlet tetrylenes, the heavy congeners of carbenes, possessing a lone pair of electrons and a vacant

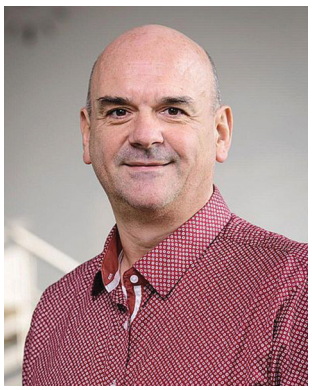

Matthias Driess

Matthias Driess is a full professor of metalorganics and inorganic materials at the Department of Chemistry of Technische Universität Berlin. He obtained his PhD degree and completed his habilitation at the University of Heidelberg in Germany. He serves as a deputy of the Cluster of Excellence UniSysCat and is a Director of the UniSysCat-BASF SE joint lab BasCat, and of the Chemical Invention Factory (CIF) for Start-ups in Green Chemistry. He is a member of the German National Academy of Sciences (Leopoldina), the Berlin-Brandenburg Academy of Sciences and Humanities, and the European Academy of Sciences.

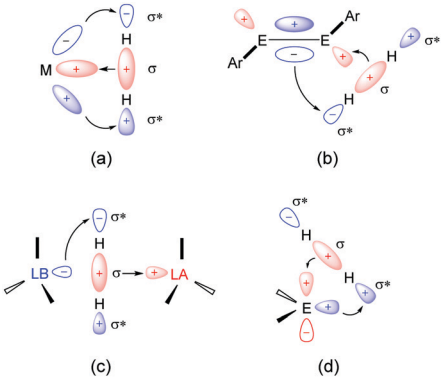

Fig. 2 Frontier orbital interactions of H_2 with (a) transition-metals, (b) multiply bonded main-group compounds, (c) frustrated Lewis pairs, and (d) carbenes and its heavy congeners, tetrylenes. Reprinted from ref. 16e with permission from AAAS, Copyright 2019.

p-orbital also show similar reactivity to transition-metal centres.[16d] The past three decades have witnessed tremendous advances in the development of isolable divalent silicon species (named silylenes) which show a fascinating reactivity towards small molecules and are even suitable for metal-free catalysis.

1.4 Divalent silicon employed in bond activation

Why using silicon for small-molecule activation? Silicon is the second most abundant element of the Earth's crust, and subvalent states (*e.g.*, Si^{II}) are well accessible. For a long time, silylenes represented laboratory curiosities and could only be studied in argon or hydrocarbon matrices at cryogenic temperatures.[21] Since the isolation of the first N-heterocyclic silylene (NHSi) reported by West and Denk,[21] a plethora of stable silylenes have been synthesised. They proved to be suitable and selectively adoptable for the activation of small molecules and metal-free catalysis. It was shown that Si^{II} species can approximate characteristics of and even become alternatives of transition metals due to its facile availability of donor/acceptor orbitals.[16] Acyclic silylenes with larger bite angles and smaller HUMO–LUMO gaps are considered as more reactive species than cyclic ones,[22] at the same time, bis-silylenes show splendid reaction scope with two Si^{II} centres synergistically interacting with substrates.[23] Examples of Si^{II}-mediated industrial transformations also show their potential for catalysis.[24] Perhaps most challenging is the regeneration of a Si^{II} site if a silylene acts as a catalyst.[16d] As several excellent reviews are available ranging from the synthesis to the reactivity of Si^{II} species,[16a–d,25] this review discusses most recent advances in the activation of H_2, CO, CO_2, N_2O, O_2, NH_3, H_2O, ethylene and P_4 by isolable silylenes and particular silylene–transition-metal complexes which show silicon–transition-metal cooperativity in the activation of bonds.

2. Isolable silylenes and their reactivity towards small molecules

2.1 Frontier orbitals for the activation of small molecules

In contrast to carbenes which can be in a triplet or singlet ground states, the Si atom in silylenes prefers the $(3s)^2(3p)^2$ valence electron configurations due to its inherent reluctance to undergo s,p-orbital hybridisation.[26] Thus, silylenes have a singlet ground state with an in-plane non-bonding lone pair of electrons featuring a high 3s-character. Accordingly, the mostly 3p out-of-plane orbital is prone to accept electrons to obey the "octet rule". Some strategies on thermodynamic and kinetic stabilisation of the reactive Si^{II} atom enables access to isolable silylenes, through introduction of heteroatoms such as N, Si and P, *etc.* and/or sterically encumbered substituents (Fig. 3). Beside the electronic and steric effects, the singlet–triplet energy differences ΔE_{ST} also account for the reactivity of silylenes. The obtuse bond angle at the Si^{II} atom leads to an increase of the p-character of the lone-pair orbital, which lowers the energy upon promoting a non-bonding lone-pair electron to a 3p-orbital.[27]

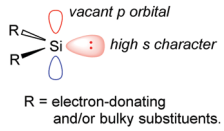

Fig. 3 Features of stabilisation in substituted silylenes.

Indeed, the modest to narrow HOMO–LUMO energy gap can be modified by combining different steric and electronic effects by the choice of suitable substituents and adjusting the angle at the Si^{II} atom.

2.2 Activation of H_2

Since the germanium alkyne analogue ArGe≡GeAr (Ar = 2,6-(2,6-$^{i}Pr_2C_6H_3)_2C_6H_3$) was shown to undergo oxidative addition with dihydrogen in 2005,[17] the activation of H_2 by other multiply-bonded main-group compounds,[15] or specific cyclic and acyclic carbenes,[18] and FLP systems[28] has also been accomplished successfully. Since the Si^{II} centre in N-heterocyclic silylenes is stabilised by the adjacent N atoms of the substituents and has a relatively small endocyclic angle, it cannot add H_2. In 2012, Jones and Aldridge reported the first room temperature-stable two-coordinate acyclic silylene **1**, bearing the strong σ-donating and high sterically demanding $B(NDippCH)_2$ substituent (Dipp = 2,6-$^{i}Pr_2C_6H_3$) (Scheme 1).[22a] This acyclic silylene undergoes facile oxidative addition of H_2, being the first example of experimentally observed dihydrogen activation by a silylene. Irreversibility of this reaction suggests it to be thermodynamically strongly exergonic ($\Delta G = -122.2$ kJ mol^{-1}), and the parallel reaction with HD gives **1-HD** as the sole product in accordance with DFT calculations which indicate a concerted bimolecular process. The computed value of $\Delta G^{\ddagger}$ (+97.2 kJ mol^{-1}) suggests a substantially lower activation energy than for other

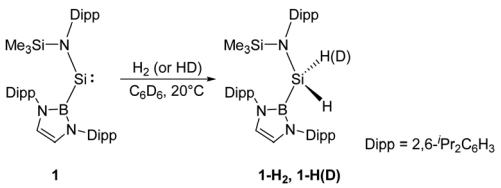

Scheme 1 H–H bond activation by the acyclic silylene **1**.

related cyclic bis(amido)silylenes. Significant widening of the bond angle at the Si^{II} atom (109.7(1)°) compared to the values for N-heterocyclic silylenes revealed a narrower singlet–triplet gap (103.9 kJ mol^{-1}) and higher reactivity, which is reminiscent of transition-metals.[29]

In the same year, Power reported another isolable acyclic silylene, $Si(SAr^{Me6})_2$ [Ar^{Me6} = C_6H_3-2,6(C_6H_2-2,4,6-Me_3)$_2$]. However, it does not react with H_2 at ambient reaction condition as the relatively high electronegativity of the thiolato substituents increases the energy gap between the lone pair and the vacant 3p orbitals of the Si atom, hampering this reaction to occur.[22b]

By taking advantage of the robust reducing agent $(thf)_2K[Si(SiMe_3)_3]$, the acyclic Si{$Si(SiMe_3)_3$}{$N(SiMe_3)Dipp$} silylene **2** was successfully isolated as purple-coloured crystals by Aldridge and co-workers (Scheme 2).[22c] Notably, the N–Si–Si bond angle of 116.91° in **2** is even larger than the corresponding N–Si–B angle of **1**. The higher degree of steric crowding in **2** is evidenced from the observation of two sets of multinuclear NMR spectra in the ratio of 1 : 1, which result from conformers related by restricted rotation along the Si–N bond. One set of the ^{1}H NMR signals is derived from the isomer in which the Dipp group lies *syn* to the hypersilyl group while the other set is due to the corresponding *anti* one. The relatively narrow energetic gap between its singlet ground state and first excited triplet state (103.7 kJ mol^{-1}) is consistent with its reactivity towards H_2 at room temperature, affording the corresponding dihydrosilane **2-H$_2$**.

In 2017, the Driess group reported that the silylene–Ni^0 complex **3** [(^{TMS}L)ClSi: → $Ni(NHC)_2$] (^{TMS}L = N-($SiMe_3$)Dipp; Dipp = 2,6-^{i}Pr$_2$$C_6H_3$, NHC = :C[(^{i}Pr)NC(Me)]$_2$) is also effective in a H_2 activation process (Scheme 3).[30] The narrow singlet–triplet gap of 77.82 kJ mol^{-1} for **3** suggests that it may be suitable for facile dihydrogen activation. Indeed, exposure of a C_6D_6 solution of **3** to H_2 atmosphere gives immediately and quantitatively **3-H$_2$**. Its ^{1}H NMR spectrum reveals the presence of both Si–H (δ 5.69 ppm) and Ni–H (δ −10.23 ppm, J(^{1}H,^{29}Si) = 16 Hz) protons as doublets. The molecular structure of **3-H$_2$** and DFT calculations suggest the initial H_2 activation occurrence at the Ni centre and the following insertion of the silylene ligand into one Ni–H bond.

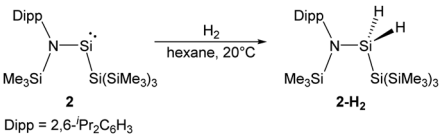

Scheme 2 Addition of H_2 to the amido(silyl)silylene **2**.

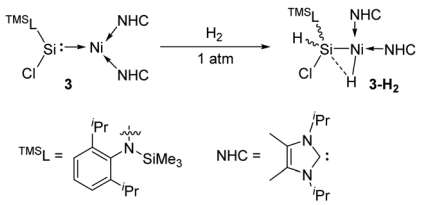

Scheme 3 Activation of H_2 by the silylene–Ni complex **3** to form **3-H$_2$**.

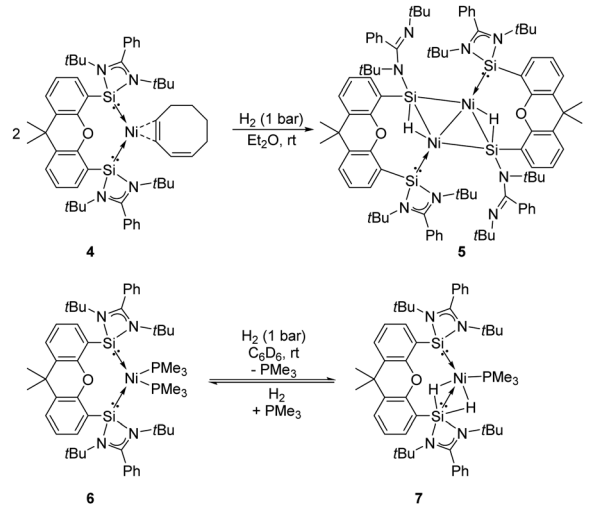

Scheme 4 Activation of H_2 by the bis-silylene–Ni complexes **4** and **6**.

The Driess group also investigated the reactivity of the bis-silylene coordinated Ni complexes [Si^{II}(Xant)Si^{II}]Ni(η^2-1,3-cod) **4** and [Si^{II}(Xant)Si^{II}]–Ni(PMe_3)$_2$ **6** towards H_2 (Scheme 4).[23f] Exposure of both Ni complexes to 1 bar H_2 at room temperature affords different kinds of activation products. The reaction of **4** with H_2 affords the unexpected diamagnetic dinuclear Ni complex **5** as yellow-brown crystals in 67% isolated yields featuring a four-membered planar Ni_2Si_2 core with two bridging hydride atoms lying almost in the same plane, whereas the reaction of **6** in a H_2 atmosphere gives the Si^{II}-stabilised Ni dihydride complex **7**. Upon removal of H_2 complex **7** converts to **6** in 29% NMR yields, suggesting a reversible H_2-activation process. Notably, the Si^{II} site plays an essential role in the activation of dihydrogen according to the DFT calculations. Indeed, the Si^{II} and Ni^0 sites show not only cooperativity in H_2 activation but also in further chemoselective hydrogenation of olefins.[23f]

The same group also reported cooperativity of Si^{II} and B^{III} in the activation of H_2: the N-heterocyclic silylene–borane complex **8** LSi-R-$BMes_2$ (L = PhC(N*t*Bu)$_2$; R = 1,12-xanthendiyl spacer; Mes = 2,4,6-$Me_3C_6H_2$), bearing a Lewis acidic boryl group, enables H_2 splitting in the style of FLP chemistry, affording the silane borane **8-H$_2$** (Scheme 5).[31] To gain further insights into the necessity of the intramolecular presence of Si^{II} and B^{III}

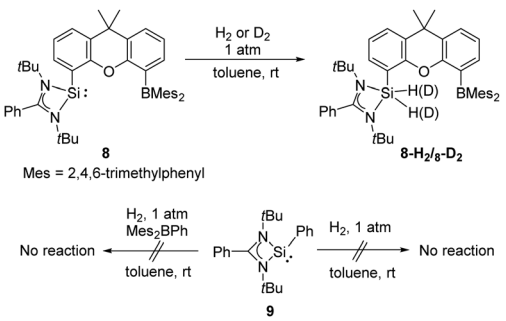

Scheme 5 Addition of H_2 by the NHSi–borane complex **8**.

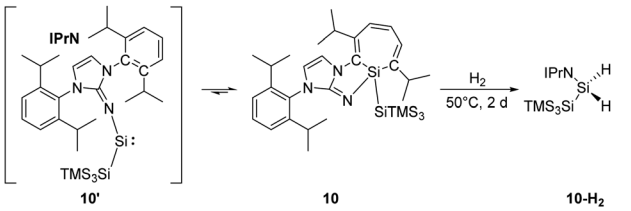

Scheme 6 Activation of H_2 by the "masked" silylene **10** to form **10-H$_2$**.

atoms for H_2 activation, the electronically similar *N*,*N*′-di-*tert*-butyl(phenylamidinato) phenylsilylene **9** as well as the intermolecular silylene borane system Mes_2BPh/**9** towards dihydrogen were both investigated. However, no hydrogenation product was observed, reflecting the importance of the indispensable role of an intramolecularly pre-organised Si–B separation in **8**.

Inoue and co-workers reported the highly reactive acyclic silylene **10**′ stabilised by an N-heterocyclic imino ligand (Scheme 6). It readily undergoes an intramolecular C=C insertion into its aromatic ligand framework, affording the room temperature stable silacycloheptatriene (silepin) **10**.[22h] Moreover, variable temperature UV-vis measurements and DFT calculations were conducted and suggested thermally accessible interconversion between silepin and silylene at higher temperatures (*e.g.* 100 °C). This equilibrium was also evidenced by isolation of a silylene–borane adduct upon addition of $B(C_6F_5)_3$. Therefore, silepin **10** acts as a "masked" silylene and takes part in the H–H bond activation process. The reaction of **10** and H_2 is slow at room temperature but leads to full conversion upon heating to 50 °C within two days. Isolation of the silane product through recrystallisation was problematic probably due to similar solubilities of all species.

More recently, the Inoue group reported the synthesis of a novel tetrasilyldisilene **11** displaying bis(silyl)silylene reactivity.[22j] Reductive debromination of $[(TMS)_3Si](tBu_3Si)SiBr_2$ with two molar equivalents of potassium graphite at low temperatures results in the formation of tetrasilyldisilene **11**, the isomer of (hypersilyl)(supersilyl)silylene **11**′ (Scheme 7). Indeed, an equilibrium between **11**′ and **11** in solutions is suggested, and the disilene/silylene equilibrium mixture is capable of H_2 activation at low temperatures. Treatment of an *n*-hexane solution of **11**/**11**′ at −40 °C with H_2 results in the quantitative formation of the corresponding silane, and no formation of the hypothetical disilene addition product is detectable. Although silylene **11**′ reacts smoothly with H_2, it exhibits a sizeable HOMO–LUMO energy gap of 403.3 kJ mol^{-1}, which contradicts the assumption that a low HOMO–LUMO gap facilitates the activation of H_2 for an acyclic silylenes. Then, further computational calculations were performed and determined a quite low effective barrier of

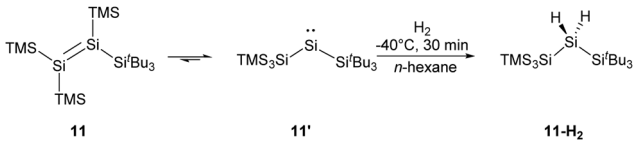

Scheme 7 Activation of H_2 by a mixture of tetrasilyldisilene **11** and bis(silyl)silylene **11**′.

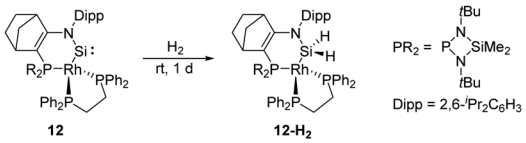

Scheme 8 Activation of H_2 by the cyclic (imino)metal substituted silylene **12**.

17.99 kJ mol^{-1}, which rationalise the reaction between **11**′ and H_2.

In 2019, Kato *et al.* isolated a cyclic (amino)metal-substituted di-coordinate silylene **12**, which is stabilised by an amino group and a Rh^I fragment (Scheme 8).[32] Interestingly, the molecular structure exhibits a distorted tetrahedral geometry around the rhodium atom rather than a classical square planar reside. A considerably shortened Si–Rh distance (2.138 Å) was observed compared to classical Si–Rh single bonds (*ca.* 2.30–2.35 Å), indicating an increased Si–Rh multiple bond character. According to theoretical calculations, geometrical deviation around the Rh centre increases the π-donating and σ-accepting character of the Rh^I fragment, which efficiently stabilises the silylene and leads to a sizeable HOMO–LUMO energy gap. However, **12** remains highly reactive towards H–H bond insertion, affording the corresponding cyclic dihydrosilane **12-H$_2$**.

More recently, Schultz *et al.* reported H_2 activation by an acyclic transient dimetallasilylene **14** $[L(Br)Ga]_2Si$: (L = HC[C(Me)-N(2,6-^{i}Pr$_2$-C$_6$H$_3$)]$_2$) (Scheme 9).[22l] **14** exhibits the lowest HOMO–LUMO energy gap (260.5 kJ mol^{-1}) and smallest ΔE_{ST} (−5.86 kJ mol^{-1}) so far, due to the kinetic and thermodynamic stabilisation by the 'metallic' LGa substituents. Therefore, it undergoes hydrogenation smoothly in the presence of H_2, otherwise giving C–C bond activation product under an inert atmosphere of argon. Notably, **14** reacts with CO to form the first isolable $[L(Br)Ga]_2Si$–CO (silylene–CO) complex (see below, Scheme 13), which acts as a "masked" silylene and activates, under liberation of CO, H_2 to give the same hydrogenation product **14-H$_2$**.

2.3 Activation of CO

Activation of CO has always been the domain of transition metals as the dissociation energy of C≡O (BDE = 1077 kJ mol^{-1}) is so high that scission of the strongest neutral triple bond is particularly challenging.[33] The well-known Fischer–Tropsch synthesis with the assistance of transition-metal catalysts involves CO bond scission in the presence of H_2.[34] On the contrary, main-group elements mediated CO activation remains rare, given its limited redox capability. Examples includes activation of CO by the highly reactive cyclic and acyclic alkyl amino carbenes to give ketenes, and germylenes to give germyloxy

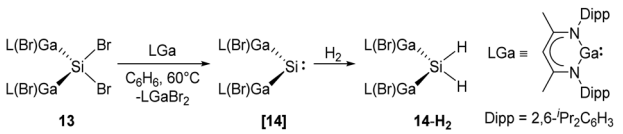

Scheme 9 Synthesis of **14-H$_2$** by the acyclic silylene **14**.

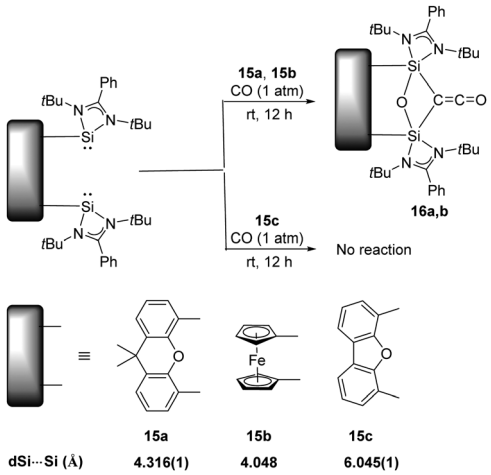

Scheme 10 Activation of CO by the bis-silylenes **15a–c**.

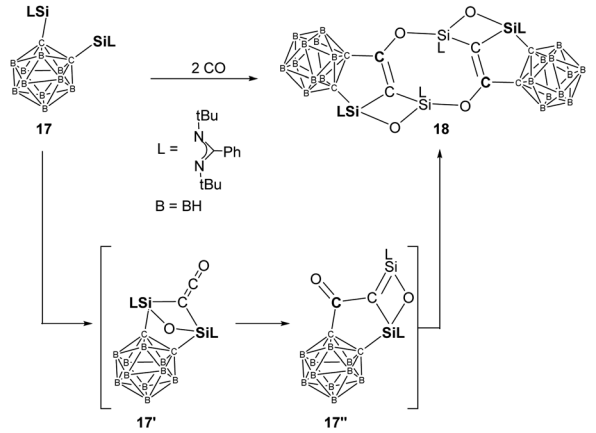

Scheme 11 Activation of CO by the bis-silylene **17**.

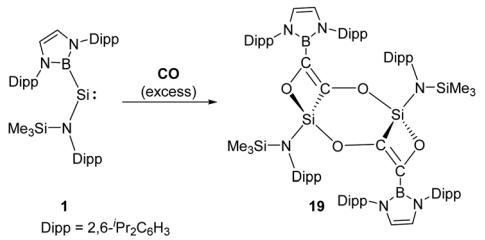

Scheme 12 Activation of CO by the acyclic silylene **1**.

ketones.[16a] Reactions with CO by other main-group species are inaccessible, presumably due to their larger HOMO–LUMO energy gap. Surprisingly, splitting and reductive homo-coupling of CO by bis-silylene $(LSi:)_2Xant$ **15a** [Xant = 9,9-dimethylxanthene-4,5-diyl; L = $PhC(NtBu)_2$] and $(LSi:)_2Fc$ **15b** (Fc = 1,1′-ferrocenyl) were reported by the Driess group (Scheme 10).[23g] Exposure of $Xant(LSi:)_2$ **15a** to CO atmosphere at room temperature for 12 hours affords $Xant(LSi)_2(\mu\text{-}O)(\mu\text{-}CCO)$ **16a** which is isolated as colourless crystals in 83% yields. A strong infrared absorption band at ν = 2069 cm^{-1} assignable to the C═O stretching vibration can be observed. In the case of **15b**, it also splits CO smoothly to afford $Fc(LSi)_2(\mu\text{-}O)(\mu\text{-}CCO)$ **16b** as confirmed by multinuclear NMR and XRD analysis. DFT calculations reveal that the initial step of CO binding and scission involved CO as a Lewis acid (four-electron acceptor), contrary to the Lewis base (two-electron donor) role during activation processes mediated by transition metals, and both silylene units of **15a** synergistically act as Lewis donors. Notably, the related bis(NHSi)dibenzofuran **15c** shows no reactivity towards CO, mainly due to the long distance between two Si^{II} atoms. In a related work, exposure of **16b** to NH_3 and benzylamine yields Fc-disiloxanediamines and respective acetamides.[35]

More recently, the same group reported another example of homocoupling of CO mediated by the bis-silylene **17** $[(LSi:)C]_2B_{10}H_{10}$ {L= $PhC(tBuN)_2$} (Scheme 11).[23h] Treatment of toluene solutions of **17** to CO atmosphere at −20 °C leads to a colour change from yellow to brown. The unprecedented head-to-tail coupling and C–O cleavage product **18** is obtained in the form of colourless crystals in 62% yields. Although the proposed disilaketene intermediate **17′** has not been isolated or even observed, DFT calculations revealed the initial formation of **17′** which undergoes migration of one C_{cage} from Si to the central C_{ketene} to afford another intermediate **17″** featuring a Si═C–C═O moiety. Head-to-tail dimerisation of **17″** furnishes the final CO homo-coupling product **18**.

Compared to N-heterocyclic silylenes, acyclic silylenes are thought to be more reactive Si^{II} species due to their more obtuse angle at silicon and narrower HOMO–LUMO gap.[27]

Aldridge *et al.* reported the reductive coupling of CO with the boryl-substituted acyclic silylene **1**, generating four- and six-membered ethynediolate **19** through the formation of intra- and intermolecular Si–O interactions (Scheme 12).[36] Notably, the reductive coupling of CO to give the ethynediolate dianion $[OCCO]^{2-}$ could only be achieved for alkali, d- and f-block metals before.[37]

Recently, the Schultz group reported the aforementioned acyclic transient dimetallasilylene **14** which reacts with CO to give the first isolable silylene carbonyl complex **20** (Scheme 13).[22l] Reaction of $[L(Br)Ga]_2SiBr_2$ **13** and one equivalent of LGa in benzene at 60 °C in CO atmosphere results in the formation of **20**. CO serves as a mild Lewis acid in the reaction while $[L(Br)Ga]_2Si$: shows strong electron-donating properties due to the electropositive L(Br)Ga substituents and the wide Ga–Si–Ga bond angle. DFT calculations were performed for the comparison of non-covalent H_2C/Si:–CO adducts. While ketene is highly favoured for carbon (−347.69 *versus* −323.84 kJ mol^{-1}), silaketene is considerably less stable than the $[H_2Si$:–CO] adduct (−44.77 *versus* −113.0 kJ mol^{-1}).

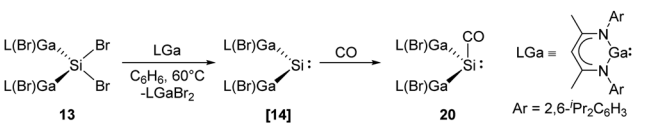

Scheme 13 Coordination of CO to the acyclic silylene **14** to form the first isolable silylene–CO complex **20**.

2.4 Activation of CO_2 and N_2O

CO_2 and N_2O activation has become a hot topic and underwent intense research due to environmental considerations. Advances involving heterogeneous, homogeneous, transition metal-free and biological catalytic systems to use CO_2 and N_2O for the formation of value-added oxygenation products have been achieved.[38,39] In main-group chemistry, multiply-bonded main-group compounds, such as disilene, and low-valent p-block compounds, such as gallium species and germylene, are also developed and found to show reactivity towards CO_2 and N_2O.[16a,c] Meanwhile, silylenes have a high oxophilicity and thus can react very efficiently with these thermodynamically very stable species.

In 1996, Jutzi *et al.* reported the first reductive activation of CO_2 with $(Me_5C_5)_2Si$ **21** under release of CO. Stoichiometric formation of the carbodisiloxane Si^{IV} complex **22** and the bis-carbonato Si^{IV} complex **23** are obtained depending on the solvent used, respectively (Scheme 14).[40] The pathway is proposed to undergo a reactive [2+1] cycloaddition intermediate or its ring-opened isomer, which easily releases CO.

In 2007, the Driess group reported the selective monooxygenation of the siloxysilylene **24** by exposing a brown solution of the siloxysilylene **24** to N_2O and CO_2 at −78 °C, respectively, affording silanoic silylester **25** in 79% yields (Scheme 15).[41] Besides, the same group reported a new NHC–silylene adduct **27** (NHC = 1,3,4,5-tetramethylimidazol-2-ylidene)[42] which undergoes facile oxygenation with N_2O to give the first isolable NHC-supported silanone **28** featuring an ylidic Si=O bond.[43] No reaction occurs between silylene **26** and N_2O even after several days at room temperature.

The Driess group also synthesised a Lewis-base coordinated Si=O complex **30** which can be obtained by oxygenation of the silylene *p*-dimethylaminopyridine (DMAP) adduct **29** with N_2O.[44] **30** was further used for the activation of ammonia, affording a unique pair of the tautomer products silahemiaminal **31** and silanoic amide **32** with DMAP being ultimately released, respectively (Scheme 16). The two products are in equilibrium in solutions, and undergo intermolecular stabilisation *via* SiOH···O=Si hydrogen bond.

The ring compound **34** featuring two four-membered disiloxane rings bridged by two oxygen atoms were synthesised by exposure of red solutions of the base-stabilised bis-silylene **33** (LSi–SiL, L = $PhC(NtBu)_2$) in toluene to N_2O at room temperature (Scheme 17).[45] A mechanism is suggested where the Si–Si bond is cleaved under insertion of an oxygen atom from N_2O. Then the two Si atoms bearing the lone pairs of electrons react with N_2O to give Si=O moieties, followed by dimerisation to give the final ring compound **34**. Meanwhile, the reaction of monosilylene **35** with N_2O affords **36** comprising a Si_3O_3 six-membered ring.[46] Unlike **34**, compound **36** features a paddle-wheel arrangement.

Kato and Baceiredo reported the phosphine-stabilised silylene **37** in 2011, which acts as either a sila-Wittig reagent or a nucleophilic silylene complex. It reduces CO_2 rapidly at room temperature, affording the original *P*-chiral tricyclic phosphine

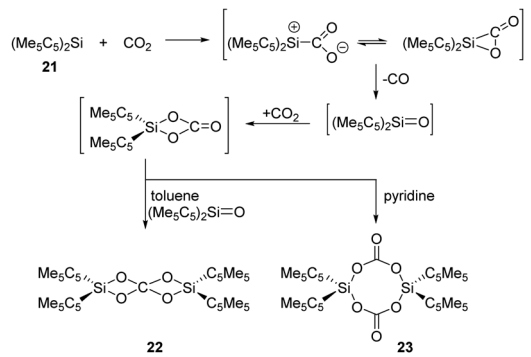

Scheme 14 Activation of CO_2 by the decamethylsilicocene **21**.

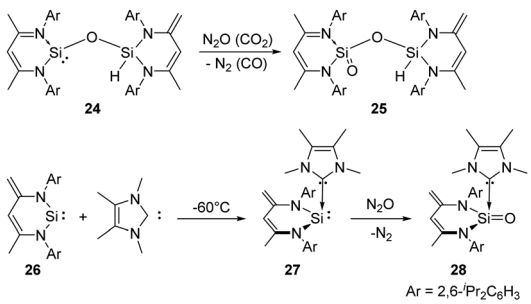

Scheme 15 Activation of N_2O/CO_2 by the siloxysilylene **24** and the NHC–silylene adduct **27**.

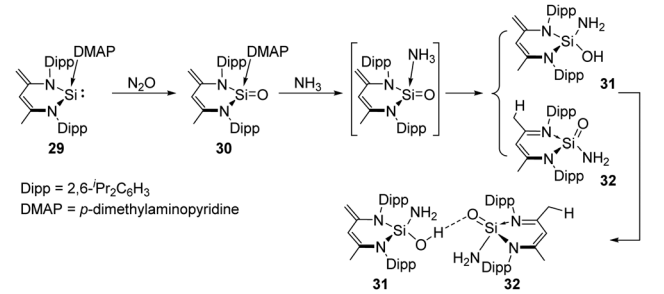

Scheme 16 Activation of NH_3 by the Si=O complex **30**.

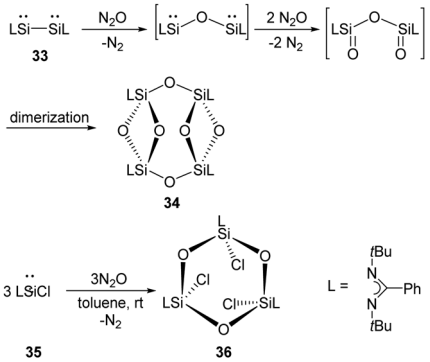

Scheme 17 Oxygenation of the mono- and bis-silylenes **35** and **33** by N_2O.

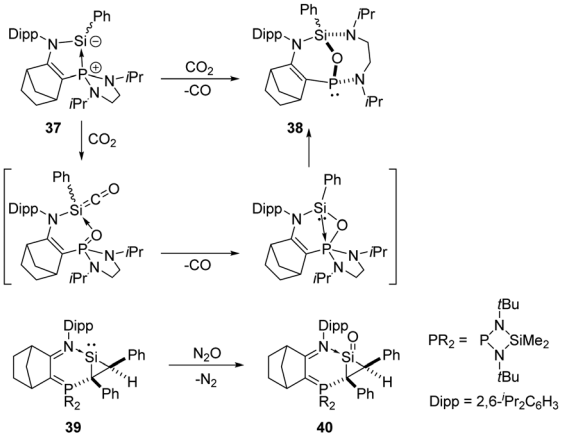

Scheme 18 Activation of CO_2 by the phosphine-stabilised silylene **37** and silacycloprop-1-ylidene **39**.

38 with an oxygen atom bridging Si and P (Scheme 18).[47] The plausible mechanism involves a phosphine centred sila-Wittig type reaction. Starting from a phosphine-stabilised silylene, the same group also synthesised the donor-stabilised silacycloprop-1-ylidene **39**,[48] and its reaction with N_2O allows access to the silacyclopropanan-1-one **40**, representing the smallest membered ring silaketone known to date.[49]

The synthesis and characterisation of the first metallosilylene **41** containing a two-coordinate silicon centre was reported by Filippou and co-workers in 2014. It shows a high reactivity towards the cleavage of the σ-bonds of H_2, H_2O, *etc.* due to the small HOMO–LUMO energy gap (Scheme 19).[50] Furthermore, exposure of **41** to N_2O gives the metallosilanone product **42**. Theoretical calculations of the σ and π NBO orbital of the Si═O bond in **42** revealed 85% of the NBO density on the O atom, suggesting a substantial contribution of a zwitterionic resonance structure (Si^{+}–O^{-}).

Kira demonstrated that the dicoordinate dialkylsilylene **43**, 2,2,5,5-tetrakis(trimethylsilyl)-silacyclopentane-1,1-diyl, reacts with CO_2 smoothly at room temperature, followed by hydrolysis by the water contamination in MeOH, to give the corresponding bis(silyl)carbonate **44** in high yields (Scheme 20).[51] DFT calculations showed that the reaction involves the formation of a Si═O bonded intermediate, which is similar to that of the decamethylsilicocene reported by Jutzi *et al.*[40]

As for the bis(amidinato)silylene **45** (Scheme 21), its reaction with an excess of N_2O at low temperatures affords the dinuclear

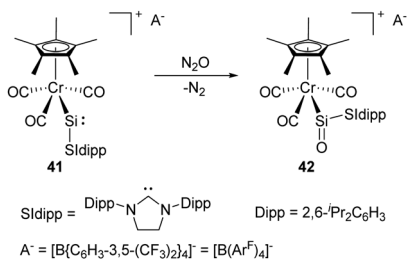

Scheme 19 Oxygenation of the metallosilylene **41** with N_2O.

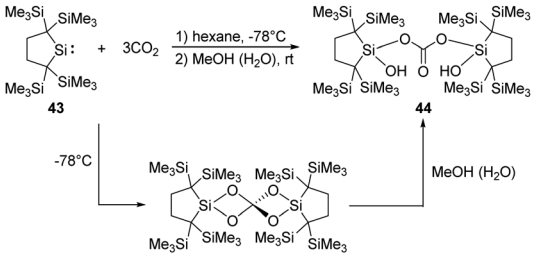

Scheme 20 Synthesis of the bis(silyl)carbonate **44** by the reaction of dialkylsilylene **43** with CO_2.

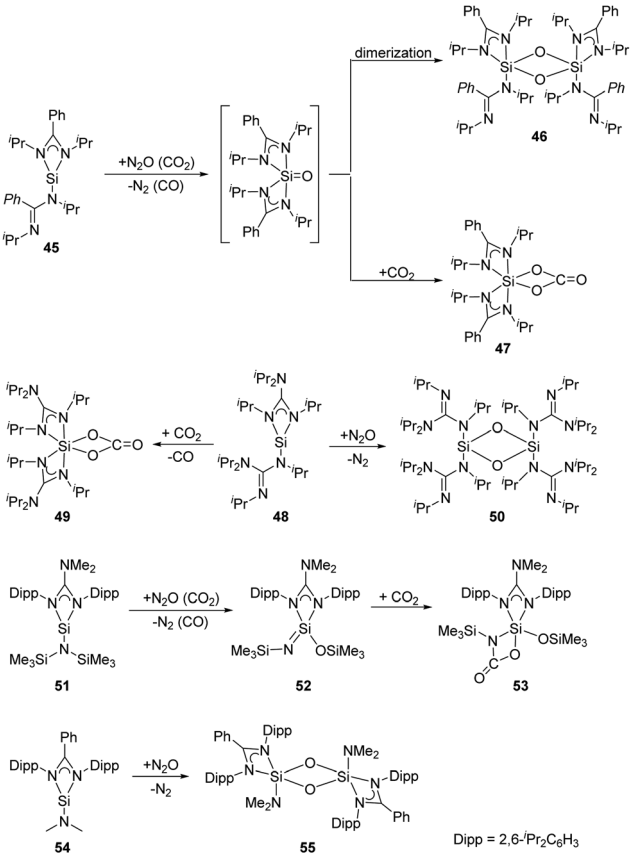

Scheme 21 Activation of N_2O and CO_2 by the amidinato silylenes **45**, **48**, **51** and **54**.

five-coordinate Si^{IV} complex **46**, while the mononuclear six-coordinate Si^{IV} complex **47** is obtained by treatment of **45** with an excess of CO_2 at room temperature.[52] The mechanism can be rationalised through the formation of a five-coordinate silanone species, followed by its dimerisation to give **46**, or reaction with an additional equivalent of CO_2 to give **47**. Similarly, treatment of the analogous bis(guanidinato)silylene **48** with N_2O and CO_2 in toluene at low temperatures affords the six-coordinate Si^{IV} complex **49** and the dinuclear four-coordinate Si^{IV} complex **50**, respectively.[53] Treatment of the guanidinatosilylene **51** with N_2O and CO_2 in toluene at low temperatures affords the unsaturated four-coordinate Si^{IV} compound **52** featuring a Si═N bond, and the five-coordinate Si^{IV}

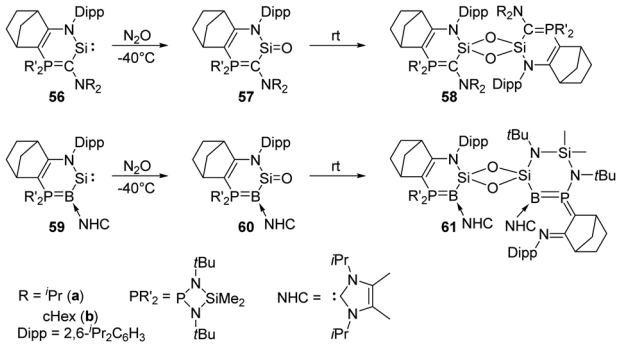

Scheme 22 Oxygenation of the phosphonium ylide and phosphonium bora-ylide silylenes **56** and **59** by N_2O.

compound **53**.[54] The silylene **54** bearing a bulky bidentate benzamidinato ligand also reacts with N_2O to give the dinuclear five-coordinate Si^{IV} compound **55**,[55] similar to those of **45** and **51**.

Heterocyclic silylene **56a** featuring a particularly electron-rich Si centre reacts smoothly with N_2O in THF at −80 °C to give the silanone product **57a** (Scheme 22), which is stable below −50 °C. However, it undergoes dimerisation at room temperature to afford the head-to-tail cyclodisiloxane **58a**, with the estimated $t_{1/2}$ being 30 min.[56] The more sterically hindered **57b** shows an enhanced persistence with $t_{1/2}$ = 5 h at room temperature. Notably, the strong electron-donating ability of the phosphonium ylide moiety is inferred to account for the electron-rich Si centre and related reactivity. Therefore, by taking advantage of the better donating ability of phosphonium bora-ylide function, the (amino)(bora-ylide)silylene **59** reacts immediately with N_2O at −20 °C to give the corresponding silanone **60**.[57] Even though the electronic effects of phosphonium bora-ylide and sterically bulky substituents play a great role for the stabilisation of silanone **60**, its dimerisation remains exergonic (ΔG_{61-60} = −66.9 kJ mol^{-1}) and furnishes slowly the cyclodisiloxane **61** at room temperature ($t_{1/2}$ = 4 d).

The ''masked'' form of acyclic silylenes, silepin **10** and its analogue **10a** (Scheme 23), demonstrated by Inoue *et al.*, also undergo oxygenation with N_2O and CO_2, and the processes follow the mechanism which is parallel to that of the aforementioned reactions.[22h,i] Exposure of *n*-hexane solutions of the silepin to N_2O atmosphere at low temperatures gives the colourless silanone compounds **62** and **62a**, and they can be further converted quantitatively to the silicon carbonate complexes **63** and **63a** at room temperature, respectively. The synthesis of **63**

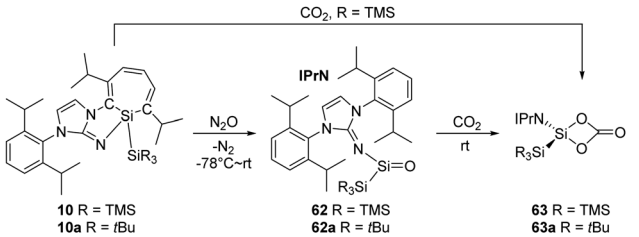

Scheme 23 Activation of N_2O and CO_2 by the acyclic silylenes **10** and **10a**.

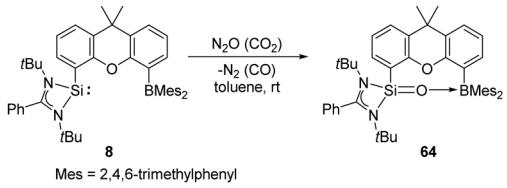

Scheme 24 Activation of N_2O and CO_2 by the silylene borane complex **8**.

can also be directly achieved by reaction of **10** with CO_2.[22h] No dimerisation of carbonato silicon compound was observed due to the bulky protection.

The silylene borane complex **8** reported by the Driess group acts as an intramolecular FLP and allows access to the silanone–borane **64** featuring a Si═O → B interaction through reductive activation of N_2O and CO_2, respectively (Scheme 24).[31] Notably, isolation of **64** is also possible *via* reaction of **8** with dioxygen.

The novel β-diketiminato-supported silaacyl chloride **66** featuring a unique Lewis-acid-free Si(O)Cl unit was synthesised by oxidation of chlorosilylene **65** with N_2O at room temperature (Scheme 25).[58] Treatment of **66** with sources of either H^- or $tBuO^-$ allows access to the nucleophilic substituted silaaldehyde **67** and silaester **68**. Analogous to the acyl chloride chemistry, silaacyl chloride **66** offers a systematic methodology to sila-carbonyl derivatives by nucleophilic substitution at the Si centre.

Another example of reductive activation of N_2O and CO_2 by the acyclic silylene **1** shows a net oxygen atom abstraction process (Scheme 26).[36] The authors inferred the formation of a short-lived silanone intermediate followed by a rapid N-to-O silyl group transfer to give the product **69**. The transition state corresponding to intramolecular silyl group transfer was identified by DFT calculations with an activation energy of 71.9 kJ mol^{-1}.

Lewis acids or bases are often introduced for the stabilisation of some reactive species. For example, Inoue *et al.* isolated

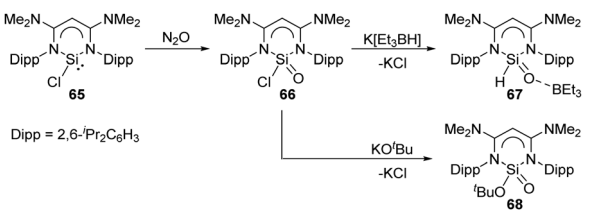

Scheme 25 Activation of N_2O by the chlorosilylene **65** and further metathesis reaction at the Si centre.

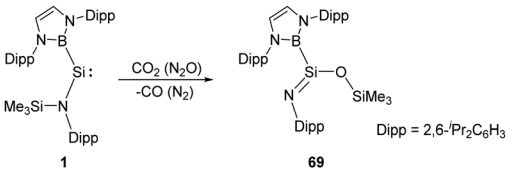

Scheme 26 Activation of N_2O and CO_2 by the acyclic silylene **1**.

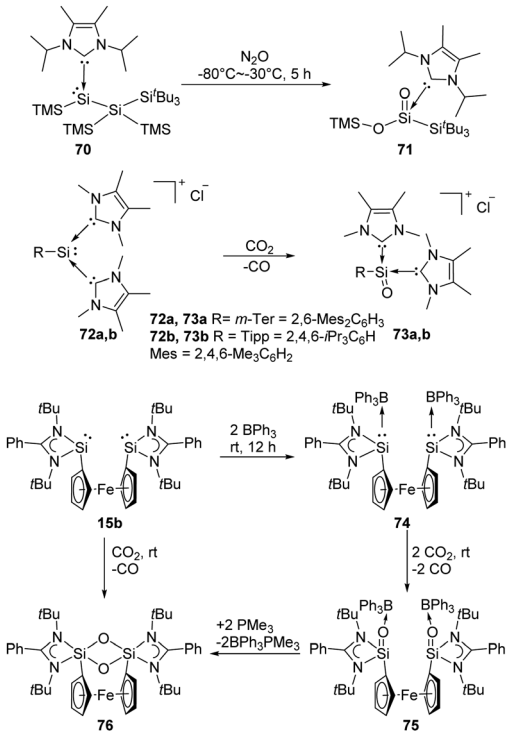

Scheme 27 Activation of N_2O and CO_2 by Lewis acid/base-stabilised Si^{II} species **70**, **72a**, **b**, **15b** and **74**.

the first acyclic NHC-stabilised silanoic ester **71** by exposure of the NHC-supported silylene **70** bearing two silyl groups to N_2O atmosphere (Scheme 27).[22j] Even though the exact mechanism is so far not clear yet, the authors inferred that the formation of a silanone with subsequent silyl migration, oxidation and rearrangement eventually lead to the ester product. The same group also reported the reduction of CO_2 using the corresponding silyliumylidene cations **72**, resulting in the successful synthesis of silaacylium ions **73** stabilised by two NHCs (NHC = 1,3,4,5-tetramethylimidazol-2-ylidene).[59] Computational calculations suggested strong Si=O bond character in **73**. Another Lewis acid-stabilised bis-silylene **15b** reported by Driess and co-workers also undergoes reductive activation of CO_2 to give silanone product **75**,[60] similar to that of intramolecular silylene borane complex **8**. Without the presence of Lewis acids, with N_2O and CO_2 the 1,3,2,4-disiloxane product **76** is obtained instead.

Recently, Iwamoto *et al.* reported the isolation of a genuine silicon analogue of a ketone, compound **78**, featuring a three-coordinate Si centre and an unperturbed Si=O bond (Scheme 28).[61] Exposing solid silylene **77** to N_2O atmosphere at room temperature affords the silanone product **78** quantitatively as a white solid. Remarkably, coordination by Lewis bases and acids or the introduction of electron-donating groups are not indispensable for this silanone case.

In 2020, Kato and Baceiredo reported the synthesis of the N-hetero-Rh^I-metallacyclic silylene **79** featuring a tetrahedral Rh centre.[62] It shows an improved stability compared with **12** and undergoes oxidation after being exposed to N_2O atmosphere at low

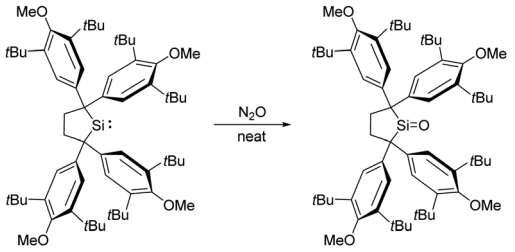

Scheme 28 Activation of N_2O by the cyclic silylene **77** to give the isolable genuine silanone **78**.

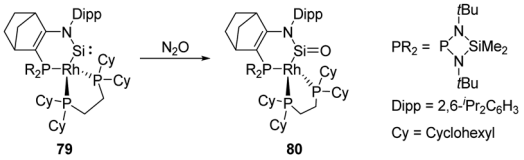

Scheme 29 Oxygenation of the cyclic (amino)(rhodium) silylene **79** by N_2O.

temperatures to furnish the corresponding silanone **80** (Scheme 29). Even though silanone **80** shows a large dimerisation energy with $\Delta G = +360.66$ kJ mol^{-1}, it displays considerable stability due to the presence of the σ- and π-donating and sterically protective Rh fragment. Cooperative involvement of both Si=O and Rh^I reactive sites was observed on its further reactivity towards H_2.

2.5 Activation of O_2

Activation of the O–O bond in dioxygen is non-trivial and crucial in both biology and industry. Nature has evolved several strategies to achieve this goal, such as cytochrome oxidase[63] and metalloenzymes taking Cu-[64] and Fe-sites[65] as cofactors. A lot of homo- and hetero-multinuclear metal complexes were also developed to achieve a controllable activation of O_2.[66] As expected by the large oxophilicity of silicon, silylenes are very reactive towards O_2.

The first isolable N-heterocyclic silylene **81** reacts with dry O_2 rapidly, giving rise to a colourless and insoluble polymer. At the same time, a small amount of minor product **82** could also be observed and verified by ^{1}H NMR data and mass spectrometry (Scheme 30).[67] However, any further characterisation was prevented due to insufficient amounts. The proposed pathway reveals the initial formation of a transient silanone, which then undergoes dimerisation to give **82**.

West *et al.* reported the new isolable silylenes **83a–b**, *rac*-*N*,*N*′-di-*tert*-butylethylene-4,5-dimethyl-1,3-diaza-2-silacyclopentan-

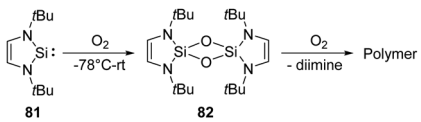

Scheme 30 Activation of O_2 by the NHSi **81**.

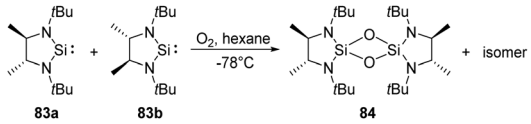

Scheme 31 Oxygenation of the NHSis **83a** and **83b** by O_2.

2-ylide (Scheme 31), which have been utilised for the reaction with a stoichiometric amount of O_2 at low temperatures, affording the corresponding 1,3,2,4-disiladioxetane.[68] Interestingly, the *meso* isomer **84** was isolated as solid, while the *rac* isomer being a colourless liquid.

On the exploration of isolable silanoic ester synthesis from the siloxysilylene **24**, its reaction with dioxygen at −78 °C readily gives an unexpected new type of strained cyclodisildioxane **85** featuring a remarkably clean deoxygenation process (Scheme 32).[41] Compounds **24′** and **24″** are assumed to be reactive intermediates during the formation of this cyclodisildioxane compound.

2,3-Dioxasilirane with a SiO_2-peroxo ring has always been elusive species for a long time and could only be generated and studied in cryogenic argon matrices. This situation has changed since Driess *et al.* reported the isolable adducts **86** and **86a** of transient dioxasilirane featuring fascinating five-coordinate square-pyramidal silicon atoms and ''side-on'' coordinated peroxo ligands (Scheme 33).[44] **86** and **86a** can be obtained selectively through facile O_2 activation with the NHC-stabilised silylenes **27** and **27a**, respectively. Remarkably, **86** undergoes internal oxygen atom transfer at room temperature to afford a cyclourea → sila-urea adduct **87** featuring a C═O → Si═O dative interaction, which highlights the importance of donor–acceptor stabilization for the successful isolation of elusive silicon–oxygen species.

The base-stabilised silacycloprop-1-ylidene **39** was reported by Kato and Baceiredo and demonstrated to react with O_2, leading to the base-stabilised sila-β-lactone product **88** featuring a planar

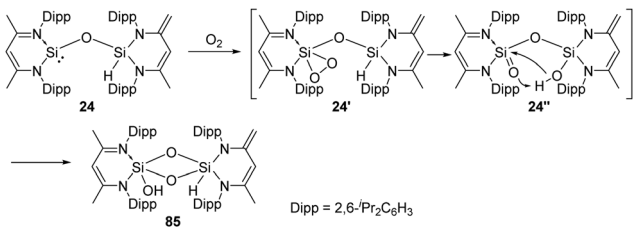

Scheme 32 Activation of the siloxysilylene **24** by O_2.

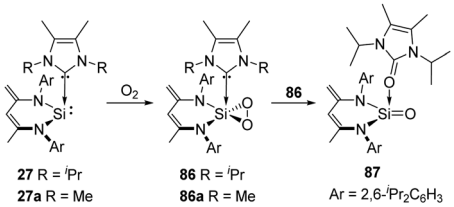

Scheme 33 Activation of O_2 by the NHC-activated silylenes **27** and **27a**.

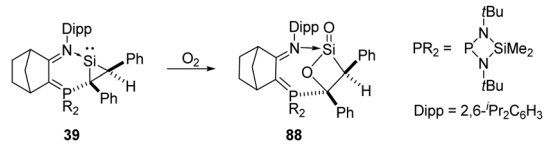

Scheme 34 Activation of O_2 by the silacycloprop-1-ylidene **39**.

β-lactone four-membered ring (Scheme 34).[69] Driven by the ring strain and the high polarity of silacarbonyl function, the reactive lactone **88** reacts with ethanol to afford donor/acceptor-stabilised silanoic acid.

As an alternative route to an acyclic silanone, Jones and Aldridge *et al.* treated the acyclic diaminosilylene **89** with an excess of dry O_2, leading to an unexpected unsymmetrical silanol **90** (Scheme 35).[22g] This reaction is assumed to proceed *via* a transient dioxasilirane followed by O–O bond cleavage and a subsequent radical-induced alkyl C–H activation, though the attempts to observe the transient silirane were unsuccessful.

2.6 Activation of H_2O, $H_2O{\cdot}B(C_6F_5)_3$ and H_2S

Activation of water is most commonly observed in nature, existing in a series of hydrolase enzymes.[70] H_2O and H_2S are also fundamental to our industrial society due to their inherent availability. Comparatively, introduction of hydroxy and sulfide can be easily achieved by relatively reactive isolable silylenes.

West and co-workers demonstrated that the first isolable N-heterocyclic silylene **81** inserts into O–H bonds of H_2O easily (Scheme 36).[71] Isolation of the colourless disiloxane **91** can be achieved from the reaction of silylene **81** with H_2O. The corresponding silanol compound is proposed to be an intermediate which eventually self-condenses to the product.

Similarly, the saturated analogue of **81**, silylene **92**, also undergoes the same insertion into O–H bond of water,

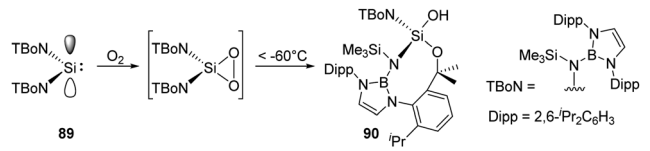

Scheme 35 Synthesis of the silanol **90**.

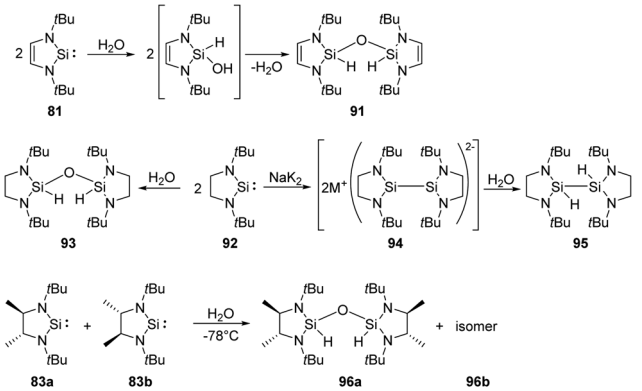

Scheme 36 Activation of H_2O by the NHSis **81**, **92**, **83a**, and **83b**.

affording disiloxane **93**.[72] Notably, the overreduction of silylene **92** competes with the reduction of its dichloro precursors, resulting in a lower yield of silylene. The overreduction product **94** can be trapped by proton abstraction from water, giving the dihydrido compound **95**. As for the racemic saturated silylenes **83a** and **83b**, both *rac* and *meso* disiloxane isomers (**96a** and **96b**) are formed, resulting from the reaction of the silylenes and H_2O *via* the corresponding silanol intermediate.[68]

The zwitterionic silylene **26** also undergoes H_2O activation in the molar ratio of 2 : 1, affording solely the siloxy silylene **98** which represents an unprecedented type of mixed-valent disiloxane compound containing di- and tetravalent silicon atoms bridged by an O atom (Scheme 37).[73] Although the mechanism is still unclear, the formation of **98** suggests a faster proton migration from a terminal methyl group in the proposed reactive intermediate **97** than from the OH group in **97′** to the divalent silicon atom. Meanwhile, the presence of a strong Lewis acid bound to oxygen atom of water leads to the drastically increased acidity of the OH group and fast proton migration from the OH group to Si. This assumption is verified by addition of the water–borane adduct $H_2O{\cdot}B(C_6F_5)_3$ to **26** in a molar ratio of 1 : 1, which affords exclusively the silaformamide–borane complex **99** featuring a unique short Si-O interatomic distance of 1.552(2) Å. IR measurements by means of isotope labelling experiments and DFT calculations were performed to verify the Si═O bond character in **99**. The observed bands for ^{18}O-labeled (1112 cm^{-1}) and ^{16}O-**99** (1165 cm^{-1}) to a Si═O stretching mode are far above frequencies typical for Si–O single bonds (800–900 cm^{-1}). Silylene **26** also shows reactivity towards H_2S at low temperatures in the molar ratio of 1 : 1, resulting in the surprisingly simple formation of the donor-stabilised silathioformamide **100**.[74]

Different from the well-studied reactions of silylene **26** with water, the addition of H_2O to complex **101** enables the donor/acceptor abilities of the silicon ligand to be tuned while still coordinated to the Ni centre and without changing its ligand sphere, affording the corresponding Si^{II} hydroxide–Ni complex **102** (Scheme 38).[75] This process is in contrast to the well-studied reactions of other metal silylene complexes with H_2O where the Si–metal bond is either broken by 1,1-addition to the Si^{II} centre or remains intact by 1,2-addition across the Si–metal bond.[76] Besides, complex **101** is also capable of activating H_2S in the molar ratio of 1 : 1, solely affording the

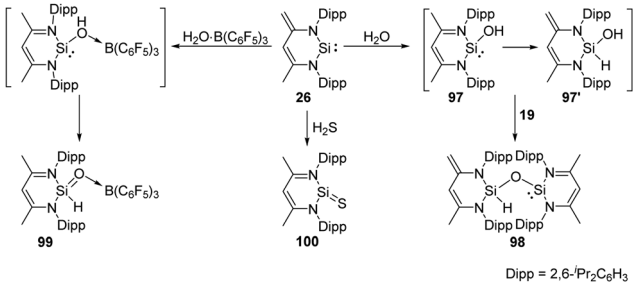

Scheme 37 Activation of H_2O, H_2S and $H_2O{\cdot}B(C_6F_5)_3$ by the zwitterion-like NHSi **26**.

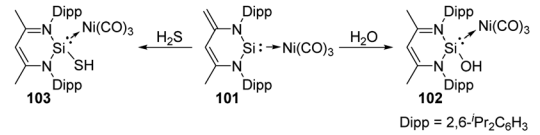

Scheme 38 Additions of H_2O and H_2S by the silylene–Ni^0 complex **101**.

1,4-addition product **103** despite the high thiophilicity of nickel.[74]

The reaction of the monochlorosilylene **35** with $H_2O{\cdot}B(C_6F_5)_3$ in the presence of IPr [1,3-bis(2,6-diisopropylphenyl)-imidazol-2-ylidene] leads to the formation of a stable silicon analogue of an acid anhydride **106** featuring an O═Si–O–Si═O core (Scheme 39).[77] The presumed mechanism reveals the involvement of a silaformaldehyde **104b** and a silacarboxylic acid **105**. The reaction of **35** and $H_2O{\cdot}B(C_6F_5)_3$ affords **104a** along with the elimination of HCl as IPr·HCl. **104b** is then obtained by subsequent rearrangement of **104a** and undergoes isomerisation to give **104c**. Oxygen abstraction of cationic silicon of **104c** affords **105**, and finally protonation of the amidinate ligand of **104b** by **105** affords finally the acid anhydride analogue **106**.

The first acyclic silacarbonyl halide compound **108** stabilised by Lewis donor was reported by Roesky *et al.* (Scheme 40).[78] **108** can be prepared by insertion of silylene **107** into the O–H bond of $H_2O{\cdot}B(C_6F_5)_3$ adduct and subsequent elimination of HCl assisted by IPr (1,3-bis(2,6-diisopropylphenyl)imidazol-2-ylidene). The stable silaformyl chloride **108** features a significant Si═O bond character and a distorted tetrahedral Si centre.

Müller *et al.* have developed a previously unknown synthetic pathway for the stabilisation of silylenes by taking advantage of

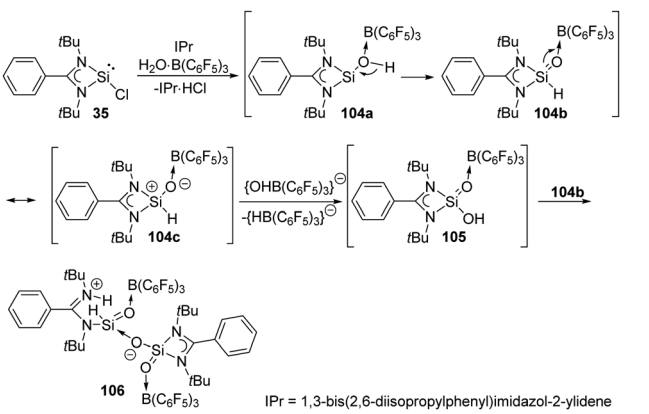

Scheme 39 Reaction of $H_2O{\cdot}B(C_6F_5)_3$ with the monochlorosilylene **35**.

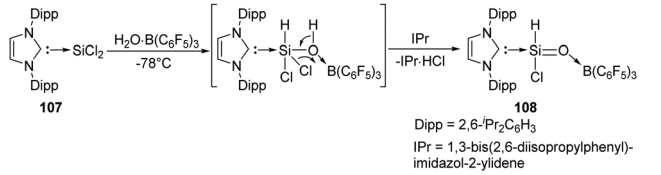

Scheme 40 Reaction of $H_2O{\cdot}B(C_6F_5)_3$ with the NHC–dichlorosilylene adduct **107**.

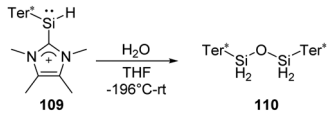

Scheme 41 Activation of H_2O by the hydridosilylene adduct **109**.

the NHC-induced fragmentation of silanorbornadiene derivatives. The new way allows the isolation and characterisation of new hydridosilylenes.[79] The hydridosilylene **109** synthesised in this way is highly reactive and shows significant reactivity after being exposed to H_2O in THF solution at low temperatures, giving cleanly the tetrahydridodisiloxane **110** as the sole product (Scheme 41).

The pre-organised intramolecular silylene borane complex **8** isolated by the Driess group acts as a FLP and undergoes unexpected metal-free dehydrogenation of H_2O to give silanone–borane **111** as an isolable product (Scheme 42).[31] Release of H_2 was observed by *in situ* ^{1}H NMR measurements with a proton resonance at δ 4.46 ppm. DFT calculations suggested that initial coordination of the H_2O molecule to the B centre forms **8A**, which further undergoes oxidation of O–H to the Si centre to yield **8B**. Subsequently, migration of OH from B to Si gives **8C**, followed by dehydrogenation to form product **111** along with release of H_2.

Synthesis and characterisation of the donor/acceptor complex of an aryl silaaldehyde **112** were demonstrated by Inoue (Scheme 43).[80] **112** can be achieved by reaction of silyliumylidene complex **72a** with an equimolar amount of H_2O at low temperatures in the presence of the Lewis acid $GaCl_3$. The proton NMR spectrum of **72a** shows a signal of Si-bound H at δ 4.98 ppm with a coupling constant of $^1J_{Si,H}$ = 234 Hz.

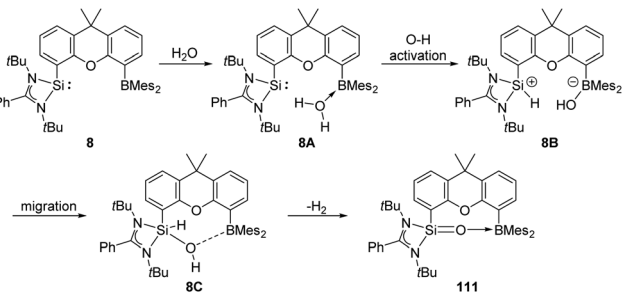

Scheme 42 Activation of H_2O by the silylene borane FLP **8**.

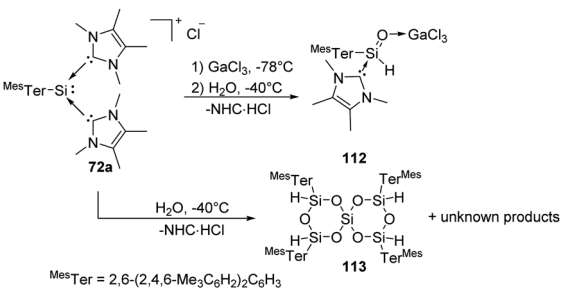

Scheme 43 Activation of H_2O by the silyliumylidene-NHC complex **72a**.

In the absence of $GaCl_3$, however, hydrolysis of silyliumylidene **72a** with the hope of isolating Lewis-acceptor free silaaldehyde resulted in the formation of a sterically hindered spirosiloxane **113** in low yields and other unknown products.

2.7 Activation of NH_3

As coordination of the Lewis base ammonia to transition-metals is more favourable, its N–H bond activation is therefore more challenging. In 2005, the first example of an intermolecular ammonia activation by a transition metal has been reported by the Hartwig group.[81] Since the activation of ammonia could also be achieved by a carbene in 2007,[18] low-valent group 13 to 15 compounds, such as digallene, germylene and phosphorus species featuring a bent geometry were found to activate ammonia.[16a,b,d] A few cyclic and acyclic silylenes also proved to be suitable for the activation of the N–H bond of ammonia. The ylide-like N-heterocyclic silylene LSi: **26** (L=CH[(C=CH_2)CMe(NDipp)$_2$]; Dipp = 2,6-^{i}PrC_6H_3), isolated by the Driess group in 2006,[73a] reacts with ammonia to afford the 1,1-addition product **114** as described by Roesky and co-workers (Scheme 44).[82] Notably, the NH_2 group in **114** is not involved in any kind of hydrogen bonding.

The silylene–Ni(CO)$_3$ complex **101** is also capable of activating ammonia and amine, affording the 1,4-addition β-diketiminato Si^{II}–Ni(CO)$_3$ complexes **115** without rupture of the Si–Ni bond or ligand exchange at the Ni atom (Scheme 44).[74] The proposed mechanism could be explained by the initial formation of an acid–base pair, increasing acidity of the N–H protons and basicity of the exocyclic methylene group. Deprotonation of N–H can then be achieved by another molecule of **101**. This process may also occur simultaneously.

Acyclic low-valent group 14 species show higher reactivity towards NH_3, for example, coordination of NH_3 to a bis(boryl) tin(II) compound followed by N–H cleavage leads to the amidotin(IV) hydride as described by Aldridge.[83] Similarly, acyclic silylenes are also good candidates for NH_3 activation. Reaction of acyclic diaminosilylene :Si(TBoN)$_2$ (TBoN = [N(SiMe$_3$){B(DAB)}]; DAB = (DippNCH)$_2$; Dipp = 2,6-^{i}Pr$_2C_6H_3$) **89** with NH_3 gives a 1 : 1 mixture of the triaminosilane **116** and the secondary amine, TBoNH (Scheme 45).[22g] The plausible mechanism reveals a transient diaminosilylene from a σ-bond

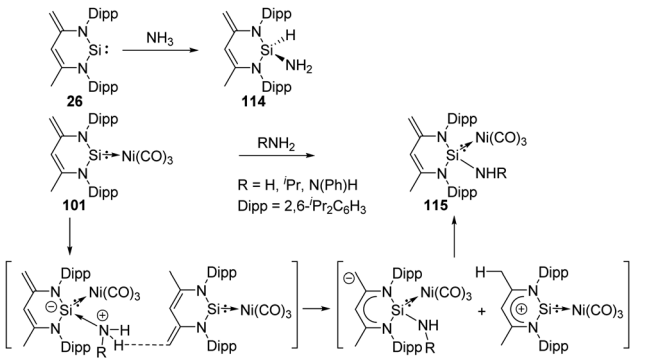

Scheme 44 Activation of NH_3 by the ylide-like NHSi **26** and its Ni complex **101**.

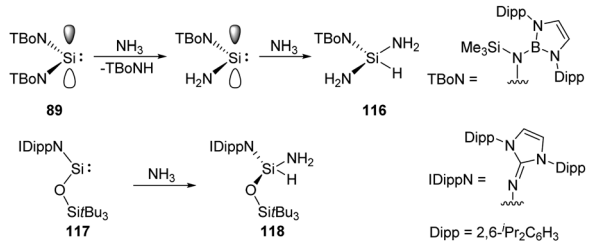

Scheme 45 Activation of NH_3 by the acyclic diaminosilylene **89** and *N,O*-silylene **117**.

metathesis reaction between **89** and NH_3, which adds NH_3 oxidatively to yield the triaminosilane product **116**. The acyclic two-coordinate *N,O*-silylene **117** also cleaves N–H bond of ammonia, affording aminosilane **118** as described by Inoue very recently (Scheme 45).[84]

The novel tetrasilyldisilene displaying bis(silyl)silylene reactivity also shows high reactivity towards NH_3. The hydroamination is achieved by treating an *n*-hexane solution of **11**/**11′** with one molar equivalent of NH_3 along with an apparent colour change from blood red to pale yellow and the formation of **119**. However, the addition product was identified by NMR spectroscopy to be only derived from tetrasilyldisilene **11** (Scheme 46).[22j]

In 2020, the Aldridge group investigated the hydroamination of $[(\text{N-nacnac})\text{Si}]^+$ **120** when being exposed to ammonia, representing the first example of oxidative addition at a two-coordinate silicon(II) cation (Scheme 47).[85] In the cases of Ge(II) and Sn(II), only Werner coordination complexes are obtained after being treated with $^t\text{BuNH}_2$. Differences in E^{II}/E^{IV} redox chemistry on descending group 14 are inferred to account for the results.

2.8 Activation of C–H bonds

C–H bond activation is one of the most potent methodologies to achieve C–C and C–heteroatom bond formation, and recent major advancement in this area has always been the domain of transition metals. Since Arduengo reported the activation of C–H bond by carbenes, some N-heterocyclic and cyclic amino carbenes are used for this purpose.[16b] With the establishment

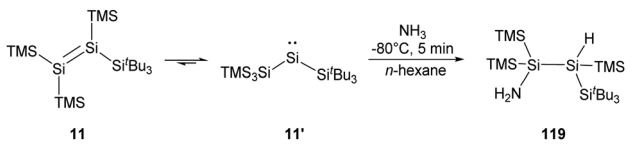

Scheme 46 Activation of NH_3 by tetrasilyldisilene **11** and bis(silyl)silylene **11′**.

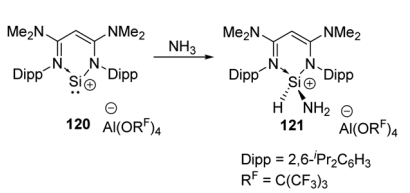

Scheme 47 Activation of NH_3 by the two-coordinate Si cation **120**.

of low-coordinate main-group chemistry, a lot of main-group species, especially silylenes, appear to be good candidates for the activation of C–H bonds. Their activation towards organic substrates might also inspire future catalytic application and narrow the catalytic gap between silylenes and transition metals.

Kira revealed that irradiation of silylene **43** with light of wavelengths longer than 420 nm allows access to the 1,1-biradical excited state (Scheme 48).[86] Thus, irradiation of **43** in the presence of mesitylene results in the insertion to a benzylic C–H bond rather than the expected silepin compound. The formation of the latter is inferred to be hampered by the steric hindrance at C=C double bonds of mesitylene.

Though aromatic C–F bond activation by N-heterocyclic silylene **26** in the absence of any additional catalyst allows access to the preparation of silicon fluorine compounds, it reacts preferentially with partially fluorinated aromatic substrates to give **123** and **124** *via* C–H bond activation (Scheme 49),[87] probably due to the weaker C–H bond.

The NHC-coordinated silylene adduct **27** (NHC = 1,3,4,5-tetramethylimidazol-2-ylidene and 1,3-diisopropyl-4,5-dimethylimidazol-2-ylidene) reported by the Driess group is found to be thermolabile and undergoes rearrangement above −20 °C, leading to the asymmetric N-heterocyclic silylcarbene **125** (Scheme 50).[88] One of the possible pathways reveals the insertion to an NMe group of NHC moiety by the reactive Si centre, followed by the cleavage of the C → Si dative bond to give the final silylcarbene product.

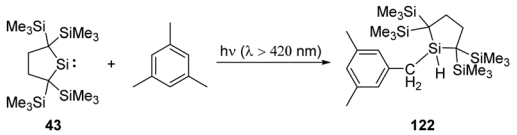

Scheme 48 Activation of a benzylic C–H bond by photochemical insertion of silylene **43**.

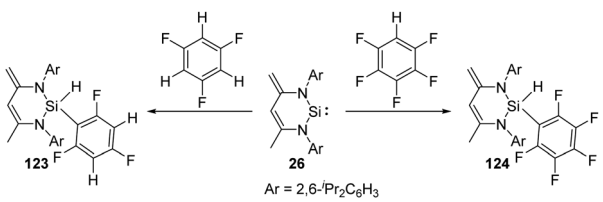

Scheme 49 Activation of aromatic C–H bond by the NHSi **26**.

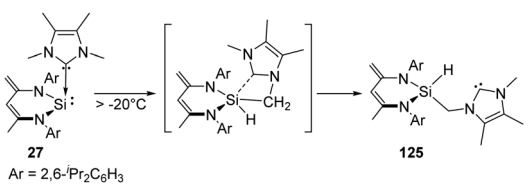

Scheme 50 Preparation of N-heterocyclic silylcarbene *via* Si-mediated activation of C–H bond with the NHC–NHSi adduct **27**.

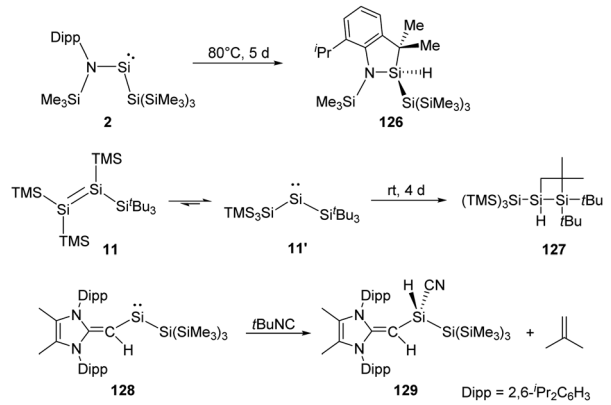

Scheme 51 Activation of C–H bond by the silylsilylenes **2**, **11′** and **128**.

Two-coordinate acyclic silylenes with narrower HOMO–LUMO energy gap compared to cyclic ones are considered as more reactive species and more likely to undergo isomerisation or intramolecular C–H bond activation. As has been discussed that $RSi(SiR_3)$ type silylenes are prone to undergo rearrangement to give isomeric disilenes, the stable acyclic silylsilylene **2** isolated by Aldridge and co-workers undergoes C–H activation over five days at 80 °C to give silaindoline **126** (Scheme 51).[22c] The bis(silyl)silylene **11′** which is in equilibrium with tetrasilyldisilene **11** *via* 1,2-silyl migrations mentioned above also undergoes intramolecular C–H activation over four days to give the full conversion to disiletane **127**.[22j] Another acyclic silysilylene **128** reported by Rivard reacts with one molar equivalent of *tert*-butyl isocyanide *via* intermolecular C–H activation, leading to the quantitative transformation of the silyl-cyanide product **129**, representing an intermolecular activation of a primary C–H bond by a silylene.[22k]

Intermolecular activation of benzylic C–H bond by silylenes is rare. Iwamoto *et al.* successfully realised a benzylic C–H insertion reaction with the cyclic (alkyl)(amino)silylene **130** in toluene solutions at elevated temperatures, furnishing hydridobenzylsilane **131** (Scheme 52).[89] Notably, the benzylic C–H insertion also competes with dehydrogenation of 9,10-dihydroanthracene by **130**, affording silanes **132**, **133** and anthracene as products.

As aforementioned, the N-hetero-Rh^I-metallacyclic silylene **12** featuring a tetrahedral Rh centre has been described by Kato and Baceiredo (Scheme 53).[32] The geometry of the Rh atom

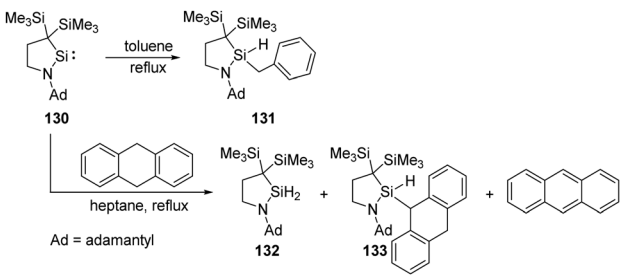

Scheme 52 Activation of benzylic C–H bond by the cyclic (alkyl)(amino)-silylene **130**.

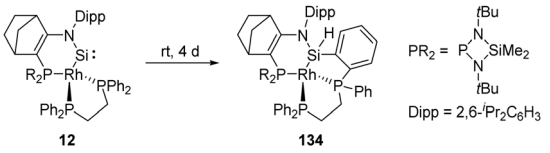

Scheme 53 Activation of intramolecular aromatic C–H bond by the metallacyclic silylene **12**.

increases the π-donating and σ-accepting character of the metal fragment, which leads to a sizeable HOMO–LUMO gap and stabilises the Si moiety. Nevertheless, **12** undergoes insertion over four days to the *ortho*-C–H bond of phenyl group bound to phosphine, furnishing the silane derivative **134**.

2.9 Activation of $CH_2{=}CH_2$

Ethylene is produced from methionine in nature and acts as an essential natural plant hormone to force the ripening of fruits.[90] It is also widely used in the chemical industry as its worldwide production exceeds that of any other raw chemicals. Major industrial reactions of ethylene include polymerisation, oxidation, halogenation *etc.* The famous Ziegler–Natta catalyst based on titanium and aluminium as active sites is extensively employed in the polymerisation of ethylene.[91] Up to now, similarly active catalysts for the polymerisation of ethylene based on silicon are still unknown. Nevertheless, a few examples for the activation of ethylene with silylenes have been reported. This includes the phosphine silylene complexes **37** and **37a** which react with ethylene to give the corresponding silirane products **135** and **135a** and the conversion is strongly dependent on the ethylene pressure (Scheme 54).[92] Notably, the two resonance signals in the ^{13}C NMR spectrum at δ −0.06 and −1.68 ppm are consistent with a silirane structure rather than a η^2-coordination mode. Interestingly this reaction shows reversibility by regeneration of the phosphine silylene **37** at low ethylene pressure. A small value of Gibbs free energy for the addition reaction was calculated [$\Delta G_{20\,°C} = (-0.717 \pm 0.452)$ kcal mol^{-1}], which shows the thermoneutrality of the reaction, in accordance with the observed reversibility of the reaction.

Reversible ethylene binding by stable, two-coordinate acyclic silylenes was also demonstrated by Power *et al.*[22e] Exposure of toluene solutions of $Si(SAr^{Me6})_2$ (Ar^{Me6} = C_6H_3-2,6(C_6H_2-2,4,6-Me_3)$_2$) **136** and $Si(SAr^{iPr4})_2$ (Ar^{iPr4} = C_6H_3-2,6(C_6H_3-2,6-$^iPr_2$)$_2$) **136a** to ethylene atmosphere results in the formation of the corresponding silirane compounds **137** and **137a**, respectively (Scheme 55). The ^{29}Si NMR spectrum of **137a** displays a signal at δ +270.7 ppm (free silylene **136a**), indicating a dissociation

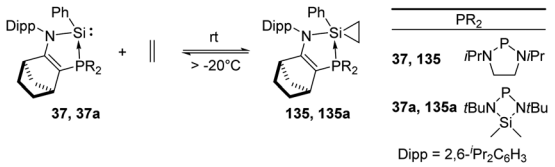

Scheme 54 Reversible addition of ethylene to the phosphine silylene complexes **37** and **37a**.

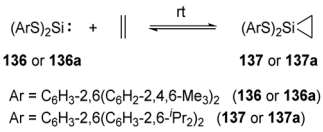

Scheme 55 Reversible addition of ethylene to the acyclic silylenes **136** and **136a**.

equilibrium in solutions. A van't Hoff analysis of the association of ethylene with **136** using variable-temperature ^{1}H NMR spectroscopy afforded $\Delta H_{assn} = -83.61(8.4)$ kJ mol^{-1} and $\Delta G_{assn} = -24.9(2.5)$ kJ mol^{-1} at 300 K, which is more favourable than that of phosphine silylene complex **37**. A van't Hoff analysis of the association of ethylene with **136a** was hampered because of the solubility characteristics of **136a** and **137a.**

Rieger *et al.* demonstrated the first migratory insertion of ethylene into a Si–Si bond in the acyclic two-coordinate silylene **2** mimicking typical reactions of transition-metal complexes (Scheme 56).[22f] A quantitative conversion to the silirane product **138**, Si{CH_2–CH_2}{NDipp($SiMe_3$)}{Si($SiMe_3$)$_3$}, is achieved at room temperature from the reaction of stable, acyclic silyl-silylene **2** in the presence of ethylene atmosphere. Upon being heated to 60 °C unexpected formation of the modified silirane Si{CH_2–CH_2}{NDipp-($SiMe_3$)}{CH_2–CH_2–Si($SiMe_3$)$_3$} **139** *via* a Si–Si bond insertion was observed. In order to investigate the mechanism, a ^{1}H NMR experiment using C_2D_4 was performed and suggested a migratory insertion of the coordinated ethylene of **138** into the Si–Si bond of the ligand and subsequent addition of a second ethylene molecule.

Inoue and Rieger *et al.* have demonstrated the reversibility between the highly reactive acyclic iminosilylsilylene **10'** and silepin **10**, which can act as a "masked" silylene.[22h] Treatment of a freshly prepared solution of silepin **10** with ethylene at room temperature affords the corresponding silirane compound **140** (Scheme 57), even though it could not be purified by crystallisation due to its similar solubility to side products. Moreover, the silirane structure can be confirmed by observation of the coupling of the central Si to the ring-bound protons in the ^{1}H–^{29}Si HMBC spectrum.

The long-term pursued acyclic and neutrally charged silanone **62a** was isolated by the Inoue group and found to perform rearrangement to give the acyclic two-coordinate *N*,*O*-silylene **117** bearing a siloxy ligand (Scheme 58).[22i] Silylene **117** undergoes

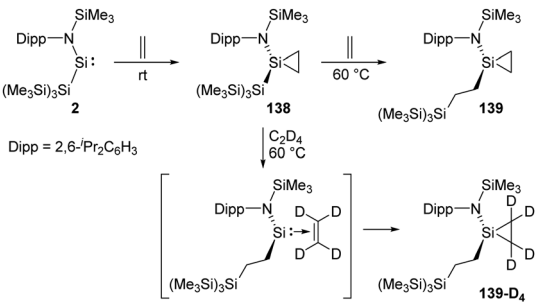

Scheme 56 Activation of ethylene by the acyclic silylene **2** *via* ethylene insertion into Si–Si bond.

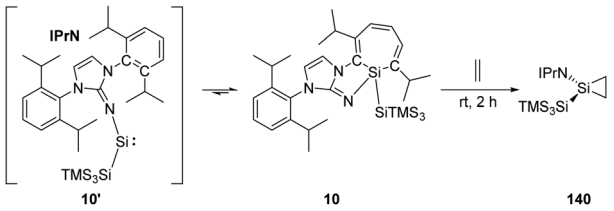

Scheme 57 Activation of ethylene by the "masked" silylene **10**.

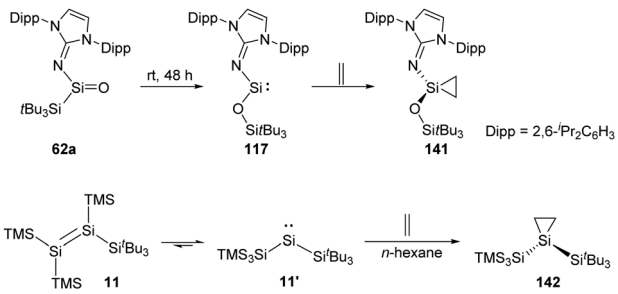

Scheme 58 Activation of ethylene by the acyclic silylenes **117** and **11'**.

irreversible transformation to give the corresponding silirane **141** when being exposed to ethylene. Irreversibility of this reaction probably benefits from the reduced steric shielding at the Si centre.[57]

Insights into the disilene–silylene equilibrium were also gained by the same group. Logically, exposure of **11** to ethylene results in the clean formation of the corresponding silirane **142** featuring an expansive Si–Si–Si bond angle of 131.7(1)° because of the steric hindrance of the silyl groups.[22j]

More recently, the reactivity of the silylene–Ni^0 complex **3** [(^{TMS}L)ClSi: → Ni(NHC)$_2$] (^{TMS}L = N-($SiMe_3$)Dipp; Dipp = 2,6-^{i}Pr$_2$C$_6$H$_3$, NHC =:C[(^{i}Pr)NC(Me)]$_2$) towards ethylene was also investigated by the Driess group (Scheme 59).[93] The addition of ethylene to **3** affords the four-membered nickelasilacyclobutane **143**. Notably, the addition reaction is reversible, and a [2+2+2] cycloaddition product, the six-membered metallasilacycle **144**, can also be achieved *via* the cleavage of the Si–Ni bond. **144** is quite unstable and undergoes a consecutive β-hydride elimination/reductive elimination to give compound **145.**

2.10 Degradation of P_4 and As_4

Phosphorus is one of the essential biogenic elements required by every living organism,[94] and phosphorus compounds play a

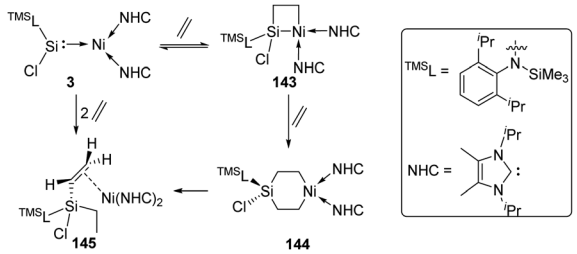

Scheme 59 Reversible activation of ethylene by the silylene–Ni complex **3**.

significant role in the industry, including ligands design, organic synthesis, drugs, optoelectronic materials and fertilisers *etc.*, due to their diverse array of useful chemical, physical and biological properties.[95] However, these phosphorus-containing species are currently prepared *via* hazardous and wasteful multi-step procedures involving the initial transformation of P_4 to PCl_3 and PCl_5.[94] Though degradation of P_4 has been established by transition-metal systems,[96] highly reactive main-group compounds also show reactivity towards P_4, for example, cyclic alkyl amino carbenes and N-heterocyclic carbenes undergo a nucleophilic attack at P_4 to give degradation products, low-valent aluminium and gallium compounds were also found to cleave P–P bonds.[16b] Silylene-mediated degradation procedures show excellent prospects due to their inherent advantages including mild conditions and easier purification processes.

In 2007, the Driess group reported the consecutive P_4 degradation with the zwitterionic silylene **26**, which results in the formation of the first SiP_4 **146** and Si_2P_4 **147** cage compounds (Scheme 60).[97] **146** can be synthesised by the reaction of **26** with P_4 in toluene in the molar ratio of 1 : 1 at room temperature and isolated in the form of colourless crystals, featuring a tricyclic SiP_4 core with pyramidally coordinated P and Si atoms in a tetrahedral environment. It bears three chemically different sorts of P nuclei according to the three temperature-invariant resonance signals (δ_X = 131.9, δ_A = −342.4, δ_B = −348.0 ppm) in the ^{31}P NMR spectrum, and the low-field resonance signal at δ_X splits into a doublet of doublets ($^1J(P_X,P_A)$ = 146.8, $^1J(P_X,P_B)$ = 144.7 Hz) while each of the two high-field signals shows a doublet of triplets ($^1J(P_X,P_A)$ = 144.7, $^1J(P_A,P_B)$ = 188.0 Hz). An X-ray diffraction analysis confirmed the molecular structure. Further reaction of **146** with silylene **26** in toluene at room temperature affords the Si_2P_4 **147** in the form of colourless crystals. The second insertion step is kinetically unfavourable due to steric congestion, and **147** shows two multiplets (δ_A = 153, δ_B = 154 ppm) in the ^{31}P NMR spectrum, representing an AA′BB′ splitting pattern of higher order with unusually small magnitudes of coupling constants.

Synthesis and characterisation of **148** featuring the planar Si–P–Si–P four-membered ring through the activation of P_4 by monochlorosilylene **35** were reported by Roesky and Stalke *et al* (Scheme 61).[98] The formation of **148** is suggested by treatment of **35** and P_4 in toluene overnight, and the structure of **148** shows a bis-ylide ring in which the two Si atoms are positively charged while the two P atoms carry partial negative charges. The natural charges obtained from the NBO analysis are +1.12 for the Si and −0.69 for the P atoms. The value of the four equivalent Si–P bonds (2.174 Å) is between a Si–P single (2.25 Å) and double bond (2.09 Å).[99] The bis-silylene **33** bearing two lone pairs of electrons and a labile Si–Si bond also reacts with P_4 at room temperature in the molar ratio of 1 : 2, affording quantitatively the same product **148**.[98] In contrast to the four-membered ring products, a neutral acyclic P_4 chain species **150** could be achieved by the degradation of P_4 with Si^{II} bis(trimethylsilyl)amido silylene **149** in toluene solutions.[100] Purple-coloured crystals can be obtained from concentrated toluene solutions at low-temperature featuring a neutral acyclic Si═P–P═P–P═Si chain with 6π electrons contained in a diphosphene and two phosphasilene units.[101] By contrast, the reaction of **149** with As_4 in toluene leads to the formation of the unprecedented As_{10} cage compound **151** featuring a nortricyclane core.[102] The Si–As bond of the exocyclic substituents in **151** can be regarded as an elongated double bond or an ion compound with the negative charge localised at the As atom and the positive charge over both N atoms in the heterocycle.

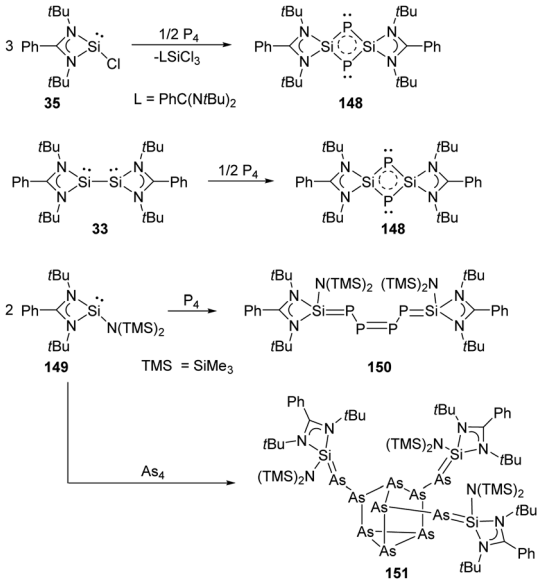

Scheme 61 Activation of P_4 and As_4 by the NHSis **33**, **35**, and **149**.

Driess and West have already investigated the reactivity of tetraaryldisilenes **152a–c**, **e** with white phosphorus and arsenic (Scheme 62).[103] The disilenes **152a–c** react with P_4 to give bicycle[1.1.0] butane compounds **154a–c**, while the more sterically encumbered disilene **152e** reacts slowly with P_4 to afford two isomers **154e** and **154e′** *via* intermediate **153**. Besides, **152a** reacts with arsenic to afford **155** and **156** in a ratio of about 3 : 1, **155** converts to **156** quantitatively when heated at 85 °C for 24 days. Comparatively, the $N(SiMe_3)_2$-substituted disilene **157** exists in equilibrium with the corresponding silylene in solutions,[104] and its reactivity towards P_4 was also investigated in a 1 : 1 molar ratio in toluene at ambient temperature, affording the Si–P cage compound **158** through the insertion of two molecules of silylenes into the P_4 tetrahedron.[101] Besides, disilene **157** also reacts with As_4 in toluene at room temperature to give $[Cp^*\{(SiMe_3)_2N\}SiAs]_2$ **159** containing a butterfly-like diarsadisilabicyclo[1.1.0]butane unit.[102]

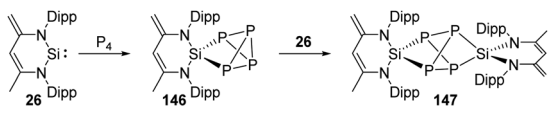

Scheme 60 Consecutive activation of P_4 by the zwitterionic NHSi **26**.

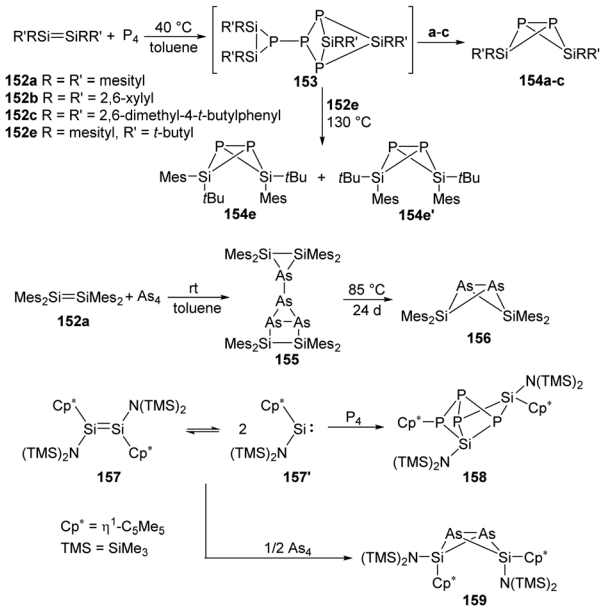

Scheme 62 Activation of P_4 and As_4 by the disilenes **152** and **157**.

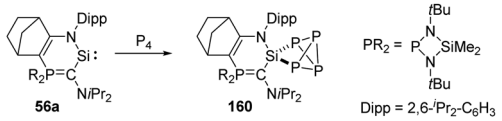

Scheme 63 Activation of P_4 by the new heterocyclic silylene **56a**.

A new isolable heterocyclic silylene **56a** stabilised by an amino group and a more π-donating and electropositive phosphonium ylide moiety was reported by Kato *et al.* (Scheme 63).[105] The silylene **56a** shows thermal stability and a robust nucleophilic character, and its reaction with P_4 occurs at room temperature *via* insertion of Si into the σ P–P bond to give the SiP_4 cage compound **160**.

While the cyclic silylene-mediated P_4 degradation is limited to the oxidative addition of a single P–P bond across the corresponding Si centre, the acyclic two-coordinate silylene **128** stabilised by a bulky vinylic N-heterocyclic olefin ligand and the σ-donating hypersilyl group shows high reactivity towards P_4 to give (^{Me}IPrCH)Si(P_4){Si($SiMe_3$)$_3$} (^{Me}IPr = [(MeCNDipp)$_2$C]; Dipp = 2,6-^{i}Pr$_2$C$_6$H$_3$) **161** as the final product (Scheme 64).[22j] The proposed mechanism probably involves the initial oxidative addition of a P–P bond followed by a subsequent 1,2-silyl migration regarding the polarised Si^{II}–Si($SiMe_3$)$_3$ bond.

More recently, the Driess group investigated the facile metal-free degradation of P_4 to the zero-valent diphosphorus complex

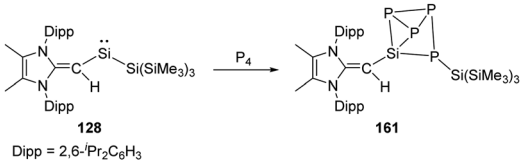

Scheme 64 Activation of P_4 by the acyclic silylene **128**.

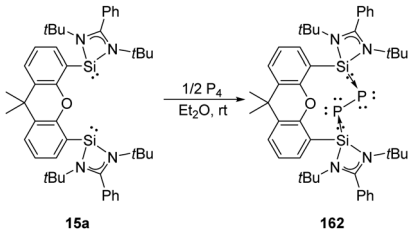

Scheme 65 Degradation of P_4 by the bis(NHSi) **15a** to give the bis-silylene-stabilised zero-valent P_2 complex **162**.

162 stabilised by two cooperative divalent Si centres of the bis-silylene **15a** (Scheme 65).[106] The two lone-pairs of electrons on each P atom in **162** allow access to facile construction of P–C, P–H and P–B bonds upon its reactions with CO_2, H_2O and a borane. Notably, **162** also serves as a monophosphorus anion (P^-) transfer reagent, leading to the phosphaketenide ligand ($P{=}C{=}O^-$) and a phosphinidene germylene complex in the presence of $M(CO)_6$ (M = Cr, W) and LGeCl (L = PhC(N*t*Bu)$_2$), respectively.

2.11 A dream in Si(II) chemistry: how to achieve fixation of N_2?

Activation of dinitrogen could so far be realised by natural nitrogenases with MoFeco[3] or industrial Haber–Bosch technology[107] under extremely high pressure and temperature. Alternative (artificial) transition-metal mediated activation of N_2 has always been laboratory curiosities since the synthesis and isolation of the first isolable transition-metal–dinitrogen complex with a (η^1-N_2) end-on coordination mode.[108] By far, numerous transition metal–N_2 complexes taking advantage of Fe,[109a–h,j,k] Mo,[109c–e,g–k] W[109d,g,h] have been developed for consecutive conversion of N_2 to ammonia, hydrazine and other fundamental nitrogen-containing chemicals.[109] Main-group elements supported fixation and functionalisation of N_2 is scarce, examples like borabenzene intermediate under flash-thermolysis condition,[110] as well as phenyl cation[111] and phenylborylene[112] under cryogenic argon matrix condition were observed by IR spectroscopy and isotopic labelling experiments. Very recently, Braunschweig and co-workers have demonstrated that coordination of N_2 to an empty 2p-orbital of a transient borylene complex gives rise to a borylene–N_2 adduct, which either reacts with the second equivalent of borylene to afford the reductive B_2N_2 product,[113] or is reduced by excess KC_8 to give a nitrene-like radical followed by dimerisation to afford a $[N_4]^{2-}$ coupling product caped with two boron centres.[114] Strong π-backbonding from boron to N_2 is revealed to be critical to end-on N_2 binding to boron atoms. Besides, Schulz has reported the isolation of an isolable silylene–CO adduct (CO is isolobal with N_2) more recently and demonstrated that the enlarged sp^2 lone pair is more available for backbonding the CO moiety ($n_{S1} \rightarrow \pi^*_{CO}$).[22l] All above examples reveal backbonding to be a critical factor for the successful fixation of N_2 as well as the weakening and functionalisation of the dinitrogen bond. Therefore, it is also inferred that modified silylenes featuring occupied and vacant orbitals proximal in space and energy can show more backbonding effects as well as play a critical role for the binding

and activation of the non-polar and strong N–N triple bond. It remains to be seen whether this summit can be reached by new tricks in silylene chemistry!

3. Conclusions and outlook

We have discussed very recent progress in small molecule activation mediated by divalent silicon without and in the presence of a transition metal. Small molecules such as H_2, CO_x, N_2O, O_2, H_2O, C_2H_4 and NH_3 are ideal and readily available resources in synthetic chemistry but require specific activation because they are constituted by relatively strong chemical bonds. Though nature has developed numerous enzymatic systems which are capable of activating most of the aforementioned small molecules but these processes are limited to physiological reaction conditions. Inspired by the latter, artificial transition-metal complexes mimicking the characteristics of metalloenzymes were developed. With the motivation of pursuing cheaper and more sustainable catalysts, heavy main-group multiply bonded compounds, FLPs and group 14 congeners of carbenes have been introduced recently, among which silylenes show an outstanding potential for metal-free activation of small molecules. The bifunctionality at the Si^{II} centre in silylenes originating from a vacant 3p orbital and a lone pair of electrons in a non-bonding orbital with high 3s character, as well a relatively narrow and tunable HOMO–LUMO energy gap are superior for mimicking transition-metal active sites. Even though in combination with transition-metals, divalent silicon centres are capable to cooperatively assist and boost bond activation and atom transfer which cannot be achieved by a transition-metal alone (*e.g.* H_2 activation and subsequent hydrogenation of olefins). Particular efforts are needed to develop suitable silylenes for the activation of extremely stable and non-polar chemical bonds, such as in N_2. Moreover, the regeneration of Si^{II} as active sites in many of the stoichiometric bond activation reactions, as herein discussed, remains challenging and key to achieve genuine low-valent silicon-based catalysis competitive to transition-metal systems.

Conflicts of interest

There are no conflicts to declare.

Acknowledgements

We thank Deutsche Forschungsgemeinschaft (DFG, German Research Foundation) under Germany's Excellence Strategy – EXC 2008/1-390540038. CS gratefully acknowledges financial support by the China Scholarship Council.

Notes and references

1 A. Holleman, E. Wiberg, N. Wiberg and G. Fischer, *Lehrbuch der anorganischen Chemie*. 2007.
2 Z. Thompson and J. A. Cowan, *Small*, 2020, e2000392.
3 (*a*) F. Mus, D. R. Colman, J. W. Peters and E. S. Boyd, *Free Radical Biol. Med.*, 2019, **140**, 250–259; (*b*) J. W. Peters and J. B. Broderick, *Annu. Rev. Biochem.*, 2012, **81**, 429–450; (*c*) P. E. M. Siegbahn, *Phys. Chem. Chem. Phys.*, 2019, **21**, 15747–15759; (*d*) R. D. Milton and S. D. Minteer, *Acc. Chem. Res.*, 2019, **52**, 3351–3360.
4 (*a*) P. M. Vignais and B. Billoud, *Chem. Rev.*, 2007, **107**, 4206–4272; (*b*) M. J. Lacasse, S. Sebastiampillai, J. P. Cote, N. Hodkinson, E. D. Brown and D. B. Zamble, *J. Biol. Chem.*, 2019, **294**, 15373–15385; (*c*) O. Lampret, J. Esselborn, R. Haas, A. Rutz, R. L. Booth, L. Kertess, F. Wittkamp, C. F. Megarity, F. A. Armstrong and M. Winkler, *et al.*, *Proc. Natl. Acad. Sci. U. S. A.*, 2019, **116**, 15802–15810.
5 (*a*) I. D. Young, M. Ibrahim, R. Chatterjee, S. Gul, F. Fuller, S. Koroidov, A. S. Brewster, R. Tran, R. Alonso-Mori and T. Kroll, *et al.*, *Nature*, 2016, **540**, 453–457; (*b*) T. Cardona, P. Sanchez-Baracaldo, A. W. Rutherford and A. W. Larkum, *Geobiology*, 2019, **17**, 127–150; (*c*) N. Cox, D. A. Pantazis and W. Lubitz, *Annu. Rev. Biochem.*, 2020, **89**, 795–820.
6 (*a*) D. C. Lamb, A. H. Follmer, J. V. Goldstone, D. R. Nelson, A. G. Warrilow, C. L. Price, M. Y. True, S. L. Kelly, T. L. Poulos and J. J. Stegeman, *Proc. Natl. Acad. Sci. U. S. A.*, 2019, **116**, 12343–12352; (*b*) V. B. Urlacher and M. Girhard, *Trends Biotechnol.*, 2019, **37**, 882–897.
7 (*a*) J. G. Rebelein, M. T. Stiebritz, C. C. Lee and Y. Hu, *Nat. Chem. Biol.*, 2017, **13**, 147–149; (*b*) M. Yuan, M. J. Kummer and S. D. Minteer, *Chem. – Eur. J.*, 2019, **25**, 14258–14266.
8 (*a*) F. Schwizer, Y. Okamoto, T. Heinisch, Y. Gu, M. M. Pellizzoni, V. Lebrun, R. Reuter, V. Kohler, J. C. Lewis and T. R. Ward, *Chem. Rev.*, 2018, **118**, 142–231; (*b*) J. M. Le and K. L. Bren, *ACS Energy Lett.*, 2019, **4**, 2168–2180.
9 M. Guo, T. Corona, K. Ray and W. Nam, *ACS Cent. Sci.*, 2019, **5**, 13–28.
10 (*a*) J. Kaplan and W. F. DeGrado, *Proc. Natl. Acad. Sci. U. S. A.*, 2004, **101**, 11566–11570; (*b*) F. Nastri, M. Chino, O. Maglio, A. Bhagi-Damodaran, Y. Lu and A. Lombardi, *Chem. Soc. Rev.*, 2016, **45**, 5020–5054; (*c*) B. Battistella and K. Ray, *Coord. Chem. Rev.*, 2020, **408**, 213176.
11 F. Moller, S. Piontek, R. G. Miller and U. P. Apfel, *Chem. – Eur. J.*, 2018, **24**, 1471–1493.
12 (*a*) M. L. Helm, M. P. Stewart, R. M. Bullock, M. R. DuBois and D. L. DuBois, *Science*, 2011, **333**, 863–866; (*b*) M. P. Stewart, M. H. Ho, S. Wiese, M. L. Lindstrom, C. E. Thogerson, S. Raugei, R. M. Bullock and M. L. Helm, *J. Am. Chem. Soc.*, 2013, **135**, 6033–6046.
13 M. T. Olsen, B. E. Barton and T. B. Rauchfuss, *Inorg. Chem.*, 2009, **48**, 7507–7509.
14 (*a*) N. S. Sickerman, K. Tanifuji, Y. Hu and M. W. Ribbe, *Chem. – Eur. J.*, 2017, **23**, 12425–12432; (*b*) F. Mus, A. B. Alleman, N. Pence, L. C. Seefeldt and J. W. Peters, *Metallomics*, 2018, **10**, 523–538.
15 P. P. Power, *Nature*, 2010, **463**, 171–177.
16 (*a*) S. Yadav, S. Saha and S. S. Sen, *ChemCatChem*, 2016, **8**, 486–501; (*b*) T. Chu and G. I. Nikonov, *Chem. Rev.*, 2018, **118**, 3608–3680; (*c*) T. J. Hadlington, M. Driess and C. Jones, *Chem. Soc. Rev.*, 2018, **47**, 4176–4197; (*d*) C. Weetman and

S. Inoue, *ChemCatChem*, 2018, **10**, 4213–4228; (*e*) R. L. Melen, *Science*, 2019, **363**, 479–484.
17 G. H. Spikes, J. C. Fettinger and P. P. Power, *J. Am. Chem. Soc.*, 2005, **127**, 12232–12233.
18 G. D. Frey, V. Lavallo, B. Donnadieu, W. W. Schoeller and G. Bertrand, *Science*, 2007, **316**, 439–441.
19 (*a*) D. Martin, M. Soleilhavoup and G. Bertrand, *Chem. Sci.*, 2011, **2**, 389–399; (*b*) M. Soleilhavoup and G. Bertrand, *Acc. Chem. Res.*, 2015, **48**, 256–266; (*c*) G. Guisado-Barrios, M. Soleilhavoup and G. Bertrand, *Acc. Chem. Res.*, 2018, **51**, 3236–3244; (*d*) S. C. Sau, P. K. Hota, S. K. Mandal, M. Soleilhavoup and G. Bertrand, *Chem. Soc. Rev.*, 2020, **49**, 1233–1252; (*e*) M. Soleilhavoup and G. Bertrand, *Chem*, 2020, **6**, 1275–1282.
20 (*a*) D. W. Stephan, *Acc. Chem. Res.*, 2015, **48**, 306–316; (*b*) D. W. Stephan, *J. Am. Chem. Soc.*, 2015, **137**, 10018–10032; (*c*) D. W. Stephan and G. Erker, *Angew. Chem., Int. Ed.*, 2015, **54**, 6400–6441; (*d*) D. W. Stephan, *Science*, 2016, **354**, aaf7229; (*e*) A. R. Jupp and D. W. Stephan, *Trends Chem.*, 2019, **1**, 35–48.
21 M. Haaf, T. A. Schmedake and R. West, *Acc. Chem. Res.*, 2000, **33**, 704–714.
22 (*a*) A. V. Protchenko, K. H. Birjkumar, D. Dange, A. D. Schwarz, D. Vidovic, C. Jones, N. Kaltsoyannis, P. Mountford and S. Aldridge, *J. Am. Chem. Soc.*, 2012, **134**, 6500–6503; (*b*) B. D. Rekken, T. M. Brown, J. C. Fettinger, H. M. Tuononen and P. P. Power, *J. Am. Chem. Soc.*, 2012, **134**, 6504–6507; (*c*) A. V. Protchenko, A. D. Schwarz, M. P. Blake, C. Jones, N. Kaltsoyannis, P. Mountford and S. Aldridge, *Angew. Chem., Int. Ed.*, 2013, **52**, 568–571; (*d*) B. D. Rekken, T. M. Brown, J. C. Fettinger, F. Lips, H. M. Tuononen, R. H. Herber and P. P. Power, *J. Am. Chem. Soc.*, 2013, **135**, 10134–10148; (*e*) F. Lips, J. C. Fettinger, A. Mansikkamaki, H. M. Tuononen and P. P. Power, *J. Am. Chem. Soc.*, 2014, **136**, 634–637; (*f*) D. Wendel, W. Eisenreich, C. Jandl, A. Pöthig and B. Rieger, *Organometallics*, 2015, **35**, 1–4; (*g*) T. J. Hadlington, J. A. Abdalla, R. Tirfoin, S. Aldridge and C. Jones, *Chem. Commun.*, 2016, **52**, 1717–1720; (*h*) D. Wendel, A. Porzelt, F. A. D. Herz, D. Sarkar, C. Jandl, S. Inoue and B. Rieger, *J. Am. Chem. Soc.*, 2017, **139**, 8134–8137; (*i*) D. Wendel, D. Reiter, A. Porzelt, P. J. Altmann, S. Inoue and B. Rieger, *J. Am. Chem. Soc.*, 2017, **139**, 17193–17198; (*j*) D. Reiter, R. Holzner, A. Porzelt, P. J. Altmann, P. Frisch and S. Inoue, *J. Am. Chem. Soc.*, 2019, **141**, 13536–13546; (*k*) M. M. D. Roy, M. J. Ferguson, R. McDonald, Y. Zhou and E. Rivard, *Chem. Sci.*, 2019, **10**, 6476–6481; (*l*) C. Ganesamoorthy, J. Schoening, C. Wolper, L. Song, P. R. Schreiner and S. Schulz, *Nat. Chem.*, 2020, **12**, 608–614.
23 (*a*) W. Wang, S. Inoue, S. Yao and M. Driess, *J. Am. Chem. Soc.*, 2010, **132**, 15890–15892; (*b*) W. Wang, S. Inoue, S. Enthaler and M. Driess, *Angew. Chem., Int. Ed.*, 2012, **51**, 6167–6171; (*c*) W. Wang, S. Inoue, E. Irran and M. Driess, *Angew. Chem., Int. Ed.*, 2012, **51**, 3691–3694; (*d*) D. Gallego, S. Inoue, B. Blom and M. Driess, *Organometallics*, 2014, **33**, 6885–6897; (*e*) Y. P. Zhou, S. Raoufmoghaddam, T. Szilvasi and M. Driess, *Angew. Chem., Int. Ed.*, 2016, **55**, 12868–12872; (*f*) Y. Wang, A. Kostenko, S. Yao and M. Driess, *J. Am. Chem. Soc.*, 2017, **139**, 13499–13506; (*g*) Y. Wang, A. Kostenko, T. J. Hadlington, M. P. Luecke, S. Yao and M. Driess, *J. Am. Chem. Soc.*, 2019, **141**, 626–634; (*h*) Y. Xiong, S. Yao, T. Szilvási, A. Ruzicka and M. Driess, *Chem. Commun.*, 2020, **56**, 747–750.
24 E. Fritz-Langhals, *Org. Process Res. Dev.*, 2019, **23**, 2369–2377.
25 (*a*) B. Blom, M. Stoelzel and M. Driess, *Chem. – Eur. J.*, 2013, **19**, 40–62; (*b*) R. Tacke and T. Ribbeck, *Dalton Trans.*, 2017, **46**, 13628–13659.
26 Y. Mizuhata, T. Sasamori and N. Tokitoh, *Chem. Rev.*, 2009, **109**, 3479–3511.
27 P. P. Gaspar, M. Xiao, D. H. Pae, D. J. Berger, T. Haile, T. Chen, D. Lei, W. R. Winchester and P. Jiang, *J. Organomet. Chem.*, 2002, **646**, 68–79.
28 G. C. Welch, R. R. San Juan, J. D. Masuda and D. W. Stephan, *Science*, 2006, **314**, 1124–1126.
29 Y. Wang and J. Ma, *J. Organomet. Chem.*, 2009, **694**, 2567–2575.
30 T. J. Hadlington, T. Szilvasi and M. Driess, *Angew. Chem., Int. Ed.*, 2017, **56**, 7470–7474.
31 Z. Mo, T. Szilvasi, Y. P. Zhou, S. Yao and M. Driess, *Angew. Chem., Int. Ed.*, 2017, **56**, 3699–3702.
32 S. Takahashi, E. Bellan, A. Baceiredo, N. Saffon-Merceron, S. Massou, N. Nakata, D. Hashizume, V. Branchadell and T. Kato, *Angew. Chem., Int. Ed.*, 2019, **58**, 10310–10314.
33 R. Kalescky, E. Kraka and D. Cremer, *J. Phys. Chem. A*, 2013, **117**, 8981–8995.
34 A. Y. Khodakov, W. Chu and P. Fongarland, *Chem. Rev.*, 2007, **107**, 1692–1744.
35 M. P. Luecke, A. Kostenko, Y. Wang, S. Yao and M. Driess, *Angew. Chem., Int. Ed.*, 2019, **58**, 12940–12944.
36 A. V. Protchenko, P. Vasko, D. C. H. Do, J. Hicks, M. A. Fuentes, C. Jones and S. Aldridge, *Angew. Chem., Int. Ed.*, 2019, **58**, 1808–1812.
37 (*a*) W. Büchner, *Helv. Chim. Acta*, 1963, **46**, 2111–2120; (*b*) S. Coluccia, E. Garrone, E. Guglielminotti and A. Zecchina, *J. Chem. Soc., Faraday Trans. 1*, 1981, **77**, 1063–1073; (*c*) P. W. Lednor and P. C. Versloot, *J. Chem. Soc., Chem. Commun.*, 1983, 284–285; (*d*) P. A. Bianconi, I. D. Williams, M. P. Engeler and S. J. Lippard, *J. Am. Chem. Soc.*, 1986, **108**, 311–313; (*e*) R. N. Vrtis, C. P. Rao, S. G. Bott and S. J. Lippard, *J. Am. Chem. Soc.*, 1988, **110**, 7564–7566; (*f*) J. D. Protasiewicz and S. J. Lippard, *J. Am. Chem. Soc.*, 1991, **113**, 6564–6570; (*g*) A. S. Frey, F. G. Cloke, P. B. Hitchcock, I. J. Day, J. C. Green and G. Aitken, *J. Am. Chem. Soc.*, 2008, **130**, 13816–13817; (*h*) P. L. Arnold, Z. R. Turner, R. M. Bellabarba and R. P. Tooze, *Chem. Sci.*, 2011, **2**, 77–79; (*i*) S. M. Mansell, N. Kaltsoyannis and P. L. Arnold, *J. Am. Chem. Soc.*, 2011, **133**, 9036–9051; (*j*) B. M. Gardner, J. C. Stewart, A. L. Davis, J. McMaster, W. Lewis, A. J. Blake and S. T. Liddle, *Proc. Natl. Acad. Sci. U. S. A.*, 2012, **109**, 9265–9270.
38 (*a*) Q. Liu, L. Wu, R. Jackstell and M. Beller, *Nat. Commun.*, 2015, **6**, 5933; (*b*) A. Cherubini-Celli, J. Mateos, M. Bonchio,

L. Dell'Amico and X. Companyó, *ChemSusChem*, 2018, **11**, 3056–3070; (*c*) X. Su, X. F. Yang, Y. Huang, B. Liu and T. Zhang, *Acc. Chem. Res.*, 2019, **52**, 656–664; (*d*) M. A. A. Aziz, A. A. Jalil, S. Wongsakulphasatch and D.-V. N. Vo, *Catal. Sci. Technol.*, 2020, **10**, 35–45.

39 (*a*) W. B. Tolman, *Angew. Chem., Int. Ed.*, 2010, **49**, 1018–1024; (*b*) E. I. Solomon, R. Sarangi, J. S. Woertink, A. J. Augustine, J. Yoon and S. Ghosh, *Acc. Chem. Res.*, 2007, **40**, 581–591.

40 P. Jutzi, D. Eikenberg, A. Möhrke, B. Neumann and H.-G. Stammler, *Organometallics*, 1996, **15**, 753–759.

41 S. Yao, Y. Xiong, M. Brym and M. Driess, *J. Am. Chem. Soc.*, 2007, **129**, 7268–7269.

42 N. Kuhn and T. Kratz, *Synthesis*, 1993, 561–562.

43 (*a*) Y. Xiong, S. Yao and M. Driess, *J. Am. Chem. Soc.*, 2009, **131**, 7562–7563; (*b*) S. Yao, Y. Xiong and M. Driess, *Chem. – Eur. J.*, 2010, **16**, 1281–1288.

44 Y. Xiong, S. Yao, R. Müller, M. Kaupp and M. Driess, *Nat. Chem.*, 2010, **2**, 577–580.

45 S. S. Sen, G. P. Tavčar, H. W. Roesky, D. Kratzert, J. Hey and D. Stalke, *Organometallics*, 2010, **29**, 2343–2347.

46 A. Jana, R. Azhakar, S. P. Sarish, P. P. Samuel, H. W. Roesky, C. Schulzke and D. Koley, *Eur. J. Inorg. Chem.*, 2011, 5006–5013.

47 D. Gau, R. Rodriguez, T. Kato, N. Saffon-Merceron, A. de Cozar, F. P. Cossio and A. Baceiredo, *Angew. Chem., Int. Ed.*, 2011, **50**, 1092–1096.

48 R. Rodriguez, T. Troadec, T. Kato, N. Saffon-Merceron, J. M. Sotiropoulos and A. Baceiredo, *Angew. Chem., Int. Ed.*, 2012, **51**, 7158–7161.

49 R. Rodriguez, T. Troadec, D. Gau, N. Saffon-Merceron, D. Hashizume, K. Miqueu, J. M. Sotiropoulos, A. Baceiredo and T. Kato, *Angew. Chem., Int. Ed.*, 2013, **52**, 4426–4430.

50 A. C. Filippou, B. Baars, O. Chernov, Y. N. Lebedev and G. Schnakenburg, *Angew. Chem., Int. Ed.*, 2014, **53**, 565–570.

51 X. Liu, X.-Q. Xiao, Z. Xu, X. Yang, Z. Li, Z. Dong, C. Yan, G. Lai and M. Kira, *Organometallics*, 2014, **33**, 5434–5439.

52 K. Junold, M. Nutz, J. A. Baus, C. Burschka, C. Fonseca Guerra, F. M. Bickelhaupt and R. Tacke, *Chem. – Eur. J.*, 2014, **20**, 9319–9329.

53 (*a*) F. M. Mück, J. A. Baus, M. Nutz, C. Burschka, J. Poater, F. M. Bickelhaupt and R. Tacke, *Chem. – Eur. J.*, 2015, **21**, 16665–16672; (*b*) F. M. Mück, D. Kloss, J. A. Baus, C. Burschka, R. Bertermann, J. Poater, C. Fonseca Guerra, F. M. Bickelhaupt and R. Tacke, *Chem. – Eur. J.*, 2015, **21**, 14011–14021.

54 (*a*) F. M. Mück, A. Ulmer, J. A. Baus, C. Burschka and R. Tacke, *Eur. J. Inorg. Chem.*, 2015, 1860–1864; (*b*) F. M. Mück, J. A. Baus, A. Ulmer, C. Burschka and R. Tacke, *Eur. J. Inorg. Chem.*, 2016, 1660–1670.

55 R. Tacke, C. Kobelt, J. A. Baus, R. Bertermann and C. Burschka, *Dalton Trans.*, 2015, **44**, 14959–14974.

56 I. Alvarado-Beltran, A. Rosas-Sanchez, A. Baceiredo, N. Saffon-Merceron, V. Branchadell and T. Kato, *Angew. Chem., Int. Ed.*, 2017, **56**, 10481–10485.

57 A. Rosas-Sanchez, I. Alvarado-Beltran, A. Baceiredo, N. Saffon-Merceron, S. Massou, D. Hashizume, V. Branchadell and T. Kato, *Angew. Chem., Int. Ed.*, 2017, **56**, 15916–15920.

58 D. C. H. Do, A. V. Protchenko, M. Angeles Fuentes, J. Hicks, E. L. Kolychev, P. Vasko and S. Aldridge, *Angew. Chem., Int. Ed.*, 2018, **57**, 13907–13911.

59 S. U. Ahmad, T. Szilvási, E. Irran and S. Inoue, *J. Am. Chem. Soc.*, 2015, **137**, 5828–5836.

60 M. P. Luecke, E. Pens, S. Yao and M. Driess, *Chem. – Eur. J.*, 2020, **26**, 4500–4504.

61 R. Kobayashi, S. Ishida and T. Iwamoto, *Angew. Chem., Int. Ed.*, 2019, **58**, 9425–9428.

62 T. Kato, S. Takahashi, K. Nakaya, A. Baceiredo, N. Saffon-Merceron, S. Massou, N. Nakata, D. Hashizume, V. Branchadell and M. F. Pastor, *Angew. Chem., Int. Ed.*, 2020, DOI: 10.1002/anie.202006088.

63 B. E. Schultz and S. I. Chan, *Annu. Rev. Biophys. Biomol. Struct.*, 2001, **30**, 23–65.

64 C. H. Kjaergaard, M. F. Qayyum, S. D. Wong, F. Xu, G. R. Hemsworth, D. J. Walton, N. A. Young, G. J. Davies, P. H. Walton and K. S. Johansen, *et al.*, *Proc. Natl. Acad. Sci. U. S. A.*, 2014, **111**, 8797–8802.

65 M. Y. Pau, J. D. Lipscomb and E. I. Solomon, *Proc. Natl. Acad. Sci. U. S. A.*, 2007, **104**, 18355–18362.

66 (*a*) H. Zhang, G. P. Hatzis, C. E. Moore, D. A. Dickie, M. W. Bezpalko, B. M. Foxman and C. M. Thomas, *J. Am. Chem. Soc.*, 2019, **141**, 9516–9520; (*b*) L. Wang, M. Gennari, F. G. Cantu Reinhard, S. K. Padamati, C. Philouze, D. Flot, S. Demeshko, W. R. Browne, F. Meyer and S. P. de Visser, *et al.*, *Inorg. Chem.*, 2020, **59**, 3249–3259; (*c*) M. L. Wind, S. Hoof, B. Braun-Cula, C. Herwig and C. Limberg, *Inorg. Chem.*, 2020, **59**, 6866–6875.

67 M. Haaf, A. Schmiedl, T. A. Schmedake, D. R. Power, A. Millevolte, J. M. Denk and R. West, *J. Am. Chem. Soc.*, 1998, **120**, 12714–12719.

68 W. Li, N. J. Hill, A. C. Tomasik, G. Bikzhanova and R. West, *Organometallics*, 2006, **25**, 3802–3805.

69 R. Rodriguez, D. Gau, T. Troadec, N. Saffon-Merceron, V. Branchadell, A. Baceiredo and T. Kato, *Angew. Chem., Int. Ed.*, 2013, **52**, 8980–8983.

70 (*a*) T. D. Bugg, *Bioorg. Chem.*, 2004, **32**, 367–375; (*b*) T. Nagasawa and H. Yamada, *Biochem. Biophys. Res. Commun.*, 1987, **147**, 701–709.

71 M. Haaf, A. Schmiedl, T. A. Schmedake, D. R. Powell, A. J. Millevolte, M. Denk and R. West, *J. Am. Chem. Soc.*, 1998, **120**, 12714–12719.

72 M. Haaf, T. A. Schmedake, B. J. Paradise and R. West, *Can. J. Chem.*, 2000, **78**, 1526–1533.

73 (*a*) M. Driess, S. Yao, M. Brym, C. van Wullen and D. Lentz, *J. Am. Chem. Soc.*, 2006, **128**, 9628–9629; (*b*) S. Yao, M. Brym, C. van Wullen and M. Driess, *Angew. Chem., Int. Ed.*, 2007, **46**, 4159–4162.

74 A. Meltzer, S. Inoue, C. Prasang and M. Driess, *J. Am. Chem. Soc.*, 2010, **132**, 3038–3046.

75 A. Meltzer, C. Präsang and M. Driess, *J. Am. Chem. Soc.*, 2009, **131**, 7232–7233.

76 M. Okazaki, H. Tobita and H. Ogino, *Dalton Trans.*, 2003, 493–506.

77 R. S. Ghadwal, R. Azhakar, H. W. Roesky, K. Propper, B. Dittrich, S. Klein and G. Frenking, *J. Am. Chem. Soc.*, 2011, **133**, 17552–17555.

78 R. S. Ghadwal, R. Azhakar, H. W. Roesky, K. Propper, B. Dittrich, C. Goedecke and G. Frenking, *Chem. Commun.*, 2012, **48**, 8186–8188.
79 D. Lutters, C. Severin, M. Schmidtmann and T. Müller, *J. Am. Chem. Soc.*, 2016, **138**, 6061–6067.
80 D. Sarkar, V. Nesterov, T. Szilvasi, P. J. Altmann and S. Inoue, *Chem. – Eur. J.*, 2019, **25**, 1198–1202.
81 J. Zhao, A. S. Goldman and J. F. Hartwig, *Science*, 2005, **307**, 1080–1082.
82 A. Jana, C. Schulzke and H. W. Roesky, *J. Am. Chem. Soc.*, 2009, **131**, 4600–4601.
83 A. V. Protchenko, J. I. Bates, L. M. Saleh, M. P. Blake, A. D. Schwarz, E. L. Kolychev, A. L. Thompson, C. Jones, P. Mountford and S. Aldridge, *J. Am. Chem. Soc.*, 2016, **138**, 4555–4564.
84 D. Reiter, P. Frisch, D. Wendel, F. M. Hormann and S. Inoue, *Dalton Trans.*, 2020, **49**, 7060–7068.
85 D. C. H. Do, A. V. Protchenko, M. A. Fuentes, J. Hicks, P. Vasko and S. Aldridge, *Chem. Commun.*, 2020, **56**, 4684–4687.
86 M. Kira, S. Ishida, T. Iwamoto and C. Kabuto, *J. Am. Chem. Soc.*, 2002, **124**, 3830–3831.
87 A. Jana, P. P. Samuel, G. Tavčar, H. W. Roesky and C. Schulzke, *J. Am. Chem. Soc.*, 2010, **132**, 10164–10170.
88 Y. Xiong, S. Yao and M. Driess, *Chem. – Asian J.*, 2010, **5**, 322–327.
89 T. Kosai, S. Ishida and T. Iwamoto, *Angew. Chem., Int. Ed.*, 2016, **55**, 15554–15558.
90 K. L. Wang, H. Li and J. R. Ecker, *Plant Cell*, 2002, **14**, S131–151.
91 A. G. Fisch, *Kirk-Othmer Encyclopedia of Chemical Technology*, J. Wiley & Sons, New York, 2019, vol. 26, pp. 502–554.
92 R. Rodriguez, D. Gau, T. Kato, N. Saffon-Merceron, A. De Cozar, F. P. Cossio and A. Baceiredo, *Angew. Chem., Int. Ed.*, 2011, **50**, 10414–10416.
93 T. J. Hadlington, A. Kostenko and M. Driess, *Chem. – Eur. J.*, 2020, **26**, 1958–1962.
94 U. Lennert, P. B. Arockiam, V. Streitferdt, D. J. Scott, C. Rodl, R. M. Gschwind and R. Wolf, *Nat. Catal.*, 2019, **2**, 1101–1106.
95 (*a*) Y. Ren and T. Baumgartner, *J. Am. Chem. Soc.*, 2011, **133**, 1328–1340; (*b*) C. Wang, M. Taki, Y. Sato, A. Fukazawa, T. Higashiyama and S. Yamaguchi, *J. Am. Chem. Soc.*, 2017, **139**, 10374–10381; (*c*) N. M. Wu, M. Ng and V. W. Yam, *Angew. Chem., Int. Ed.*, 2019, **58**, 3027–3031.
96 M. Caporali, L. Gonsalvi, A. Rossin and M. Peruzzini, *Chem. Rev.*, 2010, **110**, 4178–4235.
97 Y. Xiong, S. Yao, M. Brym and M. Driess, *Angew. Chem., Int. Ed.*, 2007, **46**, 4511–4513.
98 S. S. Sen, S. Khan, H. W. Roesky, D. Kratzert, K. Meindl, J. Henn, D. Stalke, J. P. Demers and A. Lange, *Angew. Chem., Int. Ed.*, 2011, **50**, 2322–2325.
99 (*a*) H. R. G. Bender, E. Niecke and M. Nieger, *J. Am. Chem. Soc.*, 1993, **115**, 3314–3315; (*b*) M. Driess, *Adv. Organomet. Chem.*, 1996, **39**, 193–229; (*c*) M. Driess, H. Pritzkow, S. Rell and U. Winkler, *Organometallics*, 1996, **15**, 1845–1855; (*d*) P. Pyykko and M. Atsumi, *Chem. – Eur. J.*, 2009, **15**, 12770–12779.
100 S. S. Sen, J. Hey, R. Herbst-Irmer, H. W. Roesky and D. Stalke, *J. Am. Chem. Soc.*, 2011, **133**, 12311–12316.
101 S. Khan, R. Michel, S. S. Sen, H. W. Roesky and D. Stalke, *Angew. Chem., Int. Ed.*, 2011, **50**, 11786–11789.
102 A. E. Seitz, M. Eckhardt, S. S. Sen, A. Erlebach, E. V. Peresypkina, H. W. Roesky, M. Sierka and M. Scheer, *Angew. Chem., Int. Ed.*, 2017, **56**, 6655–6659.
103 (*a*) M. Driess, A. D. Fanta, D. R. Powell and R. West, *Angew. Chem., Int. Ed. Engl.*, 1989, **28**, 1038–1040; (*b*) A. D. Fanta, R. P. Tan, N. M. Comerlato, M. Driess, D. R. Powell and R. West, *Inorg. Chim. Acta*, 1992, **198–200**, 733–739.
104 (*a*) P. Jutzi, A. Mix, B. Neumann, B. Rummel, W. W. Schoeller, H. G. Stammler and A. B. Rozhenko, *J. Am. Chem. Soc.*, 2009, **131**, 12137–12143; (*b*) S. Khan, S. S. Sen, H. W. Roesky, D. Kratzert, R. Michel and D. Stalke, *Inorg. Chem.*, 2010, **49**, 9689–9693.
105 I. Alvarado-Beltran, A. Baceiredo, N. Saffon-Merceron, V. Branchadell and T. Kato, *Angew. Chem., Int. Ed.*, 2016, **55**, 16141–16144.
106 Y. Wang, T. Szilvási, S. Yao and M. Driess, *Nat. Chem.*, 2020, DOI: 10.1038/s41557-020-0518-0.
107 V. Smil, *Nature*, 1999, **400**, 415.
108 A. D. Allen and C. V. Senoff, *Chem. Commun.*, 1965, 621–622.
109 (*a*) J. L. Crossland and D. R. Tyler, *Coord. Chem. Rev.*, 2010, **254**, 1883–1894; (*b*) N. Hazari, *Chem. Soc. Rev.*, 2010, **39**, 4044–4056; (*c*) K. C. Macleod and P. L. Holland, *Nat. Chem.*, 2013, **5**, 559–565; (*d*) H. P. Jia and E. A. Quadrelli, *Chem. Soc. Rev.*, 2014, **43**, 547–564; (*e*) Y. Nishibayashi, *Inorg. Chem.*, 2015, **54**, 9234–9247; (*f*) M. J. Bezdek and P. J. Chirik, *Angew. Chem., Int. Ed.*, 2016, **55**, 7892–7896; (*g*) Y. Tanabe and Y. Nishibayashi, *Chem. Rec.*, 2016, **16**, 1549–1577; (*h*) P. Bhattacharya, D. E. Prokopchuk and M. T. Mock, *Coord. Chem. Rev.*, 2017, **334**, 67–83; (*i*) M. Holscher and W. Leitner, *Chem. – Eur. J.*, 2017, **23**, 11992–12003; (*j*) Y. Roux, C. Duboc and M. Gennari, *ChemPhysChem*, 2017, **18**, 2606–2617; (*k*) L. J. Taylor and D. L. Kays, *Dalton Trans.*, 2019, **48**, 12365–12381; (*l*) A. J. Kendall and M. T. Mock, *Eur. J. Inorg. Chem.*, 2020, 1358–1375.
110 G. Maier, H. P. Reisenauer, J. Henkelmann and C. Kliche, *Angew. Chem., Int. Ed. Engl.*, 1988, **27**, 295–296.
111 M. Winkler and W. Sander, *J. Org. Chem.*, 2006, **71**, 6357–6367.
112 K. Edel, M. Krieg, D. Grote and H. F. Bettinger, *J. Am. Chem. Soc.*, 2017, **139**, 15151–15159.
113 M. A. Legare, G. Belanger-Chabot, R. D. Dewhurst, E. Welz, I. Krummenacher, B. Engels and H. Braunschweig, *Science*, 2018, **359**, 896–900.
114 M. A. Legare, M. Rang, G. Belanger-Chabot, J. I. Schweizer, I. Krummenacher, R. Bertermann, M. Arrowsmith, M. C. Holthausen and H. Braunschweig, *Science*, 2019, **363**, 1329–1332.

